Review on Growth and Characterization of Nonlinear Optical Organometallic Thiocyanate Crystals

Tejaswi Ashok Hegde, Atanu Dutta, Vinitha Gandhiraj*

Division of Physics, School of Advanced Sciences, Vellore Institute of Technology, Chennai, India

Received 28 August 2018; received in revised form 13 November 2018; accepted 31 January 2019

Abstract

Combinations of an inorganic distorted polyhedron with asymmetric conjugate organic molecules yield the organometallic compounds. Among them, organic thiocyanate crystals have attracted a great deal of attention for nonlinear optical device applications. The bimetallic thiocyanates of the type $AB(SCN)_4$ for example, $ZnCd(SCN)_4$, $ZnHg(SCN)_4$, $MnHg(SCN)_4$, and $CdHg(SCN)_4$ are extremely interesting for optoelectronic applications. This article highlights present knowledge on growth parameters, physicochemical properties and nonlinear optical properties of several organometallic thiocyanate crystals. The chemical property and physical stability of these materials are compared, and the best results based on the review were reported. Information about the parameters, which are necessary for crystal growth has been summarized.

Keywords: crystal growth, nonlinear optical, organometallic, bimetallic thiocyanate, single crystal, Z-Scan

1. Introduction

The process of conventional crystal growth fosters several empirical properties that often end up with optimized product quality, application efficiency, cost-effectiveness, and user-friendliness. The physicochemical and Nonlinear Optical (NLO) properties are the key parameters in developing the acceptable device grade crystals, and is likely to be used in light-emitting devices, dosimeter, and photonics, electro-optical devices, semiconductor devices, etc. [1-4]. The research has been focused on growing the nonlinear photonic crystals with lower UV cutoff, wider transmittance range, larger nonlinearity, higher damage threshold, moderate thermal and mechanical properties. Pure organic and inorganic materials have been used for growing crystals to complement each other's properties. The growth of organic crystals has become the focus of research in recent times due to the lower cost, faster nonlinear response over a wide range of frequency and higher optical damage threshold [5-17]. However, they suffer from problems such as volatility, low thermal stability and poor mechanical properties [1, 18-19].

The organometallic crystals for optoelectronic applications were brought in to practice in the late 1960s to overcome the physicochemical instabilities of organic crystals. Organometallic materials can be synthesized based on the idea of combining the inorganic distorted polyhedron with asymmetric conjugate organic molecule [2-3]. These crystals possess high optical nonlinearity and mechanical flexibility with temporal and thermal stability and excellent transmittance, unlike individual organic or inorganic crystals. A unique metal-ligand and intra-ligand charge transfer property in organometallic materials make them a promising candidate for NLO applications [2-3, 19-21].

In organometallic thiocyanate crystals, major nonlinearity arises due to the delocalized π-electrons of metal-ligand bonds. The diversity in central metal atoms, oxidation sates, size and nature of the ligand are also supportive highlights in

* Corresponding author. E-mail address: vinitha.g@vit.ac.in

tailoring materials for the increased NLO properties. An endeavor towards increasing the NLO properties of the crystals reveal the fact that the Lewis-based adducts of organometallic crystals possess better NLO properties than its parental thiocyanate (SCN) crystals [1, 22-25].

Recently, Organometallic Thiocyanate (OMT) crystals of the type $AB(SNC)_4$ with A=Zn, Co, Ni, Cd, and B=Cd, and Hg satisfied the majority of the requirements for being an efficient NLO crystal, and have attracted attention of the crystallographers. Infinite two or three-dimensional bridges, which connect A and B atoms of the inorganic compound, makes the thiocyanate based organometallic crystals more stable. The infinite network implies relatively large polarization, which causes the invisible nonlinearities in the materials [26-28]. Notably, nucleation and orientation control during the bulk crystal growth are the key parameters that influence on nonlinear optical efficiency of the crystals.

The ambidentate SNC ion can act as a bidentate binding ligand satisfying the coordination number of the metal. An insight review of the coordination behavior of the bimetallic complexes which are in the form of $AB(SCN)_4.nH_2O$ reveals the truth that it is much more complicated. In addition to this as all these compounds are synthesized in water, the coordination of water molecule with metal ions through O atom is also possible. Further, most of these Structure Type Crystals (SCN) are found to be crystallized in a centrosymmetric space group, which minimizes their macroscopic properties. This demerit leads to the basic quest of non-centrosymmetricity in the engineering of organometallic NLO crystals [23, 29-30]. It is important to mention here that only II-B metal complexes of Zn, Cd, Hg, and Mn crystallize in the non-centrosymmetric space group [19]. Furthermore, we restrict our review only to the organometallic thiocyanate crystals which were exposed as promising materials exhibits excellent NLO and mechanical properties in the literature.

This review provides an account of detailed synthesis and different properties of organometallic thiocyanate crystals. The growth parameters and certain important properties of these organometallic crystals are discussed with an emphasis on nonlinear optical properties.

2. Experimental Details

2.1. Synthesis route

Most of the organometallic thiocyanate crystals discussed here were grown in different stoichiometric compositions by solution growth method, in particular by temperature lowering/slow cooling method and slow evaporation method unless otherwise specified. Generally, we classified the synthesis and growth of organometallic thiocyanate crystals into two major types as depicted in Fig. 1. Synthesis and growth of bimetallic thiocyanate, particularly, Manganese Mercury Thiocyanate (MMTC), Zinc Mercury Thiocyanate (ZMTC), Cadmium Mercury Thiocyanate (CMTC), and Zinc Cadmium Thiocyanate (ZCTC) etc., follow one folded mechanism unlike the crystals were grown by its derivatives. A common difficulty in the growth of bulk OMT single crystals is its high solubility in an aqueous medium. However**,** it can be overcome by the introduction of different additives viz., Dimethyl Sulphoxide (DMSO), Dimethyl Acetamide (DMA), N-Methyl Pyrrolidone (NMP), and Glycol Monomethyl Ether (GME) that would yield new and efficient NLO materials. The bulk crystals synthesized in such a way are referred as derivatives of the bimetallic thiocyanate complexes.

Parameters like pH, solubility, metastable zonewidth, induction period and growth rate measurements affect the growth of the crystals. pH of the supersaturated solution plays an important role in the growth of thiocyanate complex crystals. It has been found that lower pH values lead to the formation of translucent crystals of smaller size whereas higher pH values in the range of 2.8 to 3.5 lead to good quality crystals [26, 31]. Since the crystal growth rate depends on the solubility and temperature, the solubility of the compound in different solvents need to be tested for optimizing growth parameters [23]. Metastable linewidth measurements provide the information of the stability of solution in its supersaturated region which is considered as an essential parameter for the growth of a large single crystal from the solution [32-33]. The

major influential factors on the metastable zonewidth which is an experimentally measurable quantity are the stirring rate, the cooling rate of the solution and presence of additional impurities. The induction period is defined as the measure of nucleation rate in the supersaturated solution and this is also an experimentally measurable quantity [34]. As far as the authors know, the majority of literature did not provide relevant numerical values for the induction period. To summarize, the growth rate of the crystal plane is defined as a function of a set of crystal growth parameters like temperature, the degree of supersaturation of the solution, pH, concentration of the impurities in solution and their physicochemical properties [35]. This can be represented by the equation $R = F(t, S, pH, C)$ where R represents the growth rate of the crystal, t is the temperature, S and C are the supersaturation and concentration of impurities in the solution respectively [36]. Most likely the growth rate is calculated by the weighing method proposed by Kubota et al., [32, 37]. This method defines the growth rate of crystals as $G_g = (m - m_\circ)/(m_\circ \Delta\theta)$, where m_0 is the initial mass of the crystal (Kg), m is the final mass of the crystal (Kg) and $\Delta\theta$ is the growth time. The purity of the crystal can be ascertained by repeated recrystallization of the grown crystals. (typically 2 to 3 times) [38]. Table 1 shows the set of OMT crystals grown by different growth methods, growth time and approximate sizes of the grown crystal.

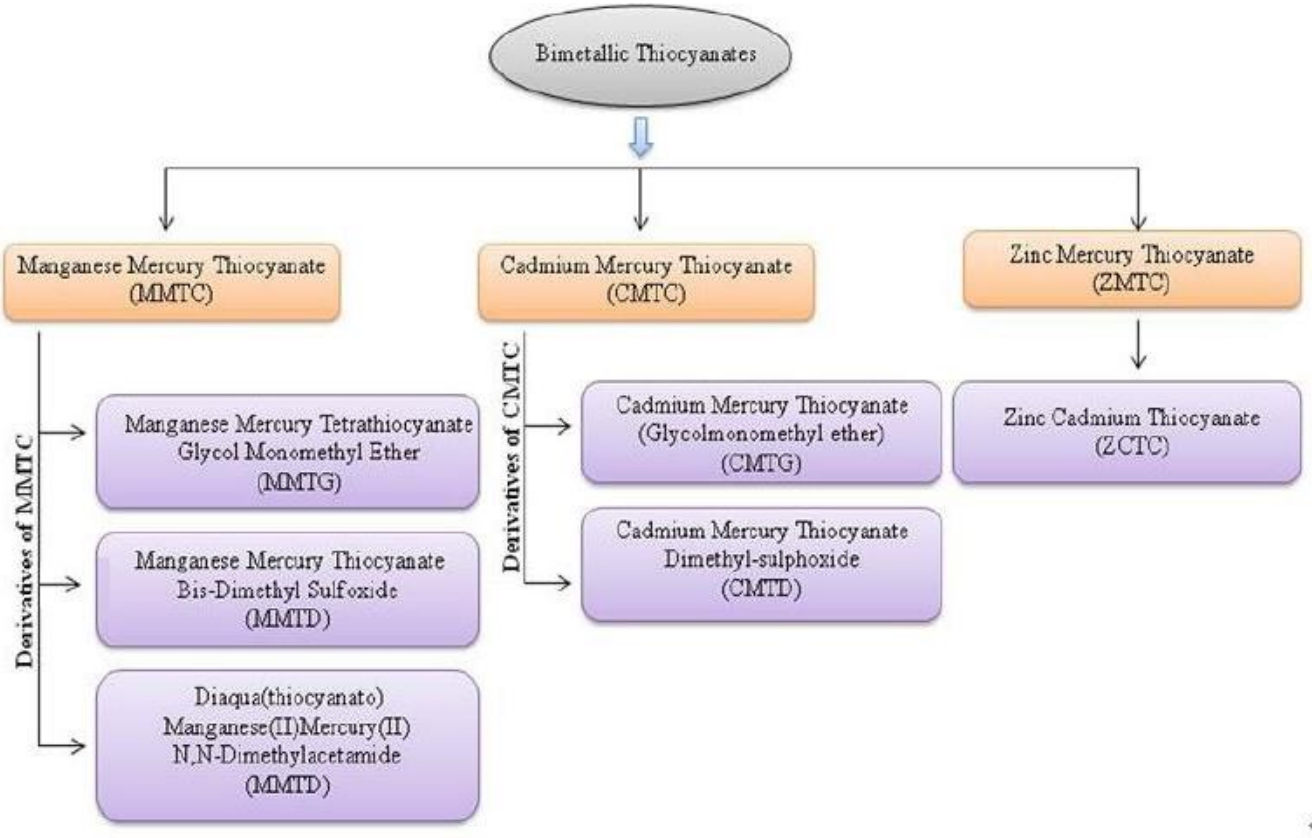

Fig. 1 The classification tree of organometallic thiocyanate crystals

Since the parameters been discussed above differ from different bimetallic thiocyanate compounds (quantitative difference), the following explains the same for different bimetallic thiocyanate compounds.

2.1.1. Synthesis of manganese mercury thiocyanate (*MMTC*)

Manganese mercury thiocyanate (MMTC) can be synthesized in different ways. The synthesis reactions that take place in the first process are as follows (where A=NH_4, Na, K) [2],

$$\begin{aligned} &2NH_4SCN + Ba(OH)_2 \rightarrow Ba(SCN)_2 + 2NH_3 \uparrow + 2H_2O \\ &Ba(SCN)_2 + MnSO_4 \rightarrow BaSO_4 \downarrow + Mn(SCN)_2 \\ &2ASCN + Hg(NO_3)_2 + Hg(SCN)_2 \rightarrow MnHg(SCN)_4 \end{aligned} \quad (1)$$

The second synthesis reaction is as follows (where X=NO_3, Cl) [2, 19].

$$\begin{aligned} &4ASCN + HgX_2 \rightarrow A_2Hg(SCN)_4 + 2AX \\ &A_2Hg(SCN)_4 + MnX_2 \rightarrow MnHg(SCN)_4 + 2AX \end{aligned} \tag{2}$$

Generally, by considering A=NH4 and X=Cl, it can be written as;

$$4NH_4SCN + MnCl_2 + HgCl \rightarrow MnHg(SCN)_4 + 4NH_4Cl \tag{3}$$

The second synthesis method is the most widely reported in the literature due to its ease of synthesis process and excellent yield compared to the first one. Under optimized composition and conditions of the precursor materials, good quality crystals of dimensions up to (14×12×11) mm^3 [2, 38-39] were obtained.

2.1.2. Synthesis of zinc mercury thiocyanate (*ZMTC*)

The growth of zinc mercury thiocyanate single crystal was carried out by a single diffusion method in silica gel [18, 40]. The reaction scheme in a gel medium can be written as follows;

$$ZnCl_2 + 4NH_4SCN + HgCl_2 \rightarrow \mathrm{ZnHg(SCN)_4} + 4NH_4Cl \tag{4}$$

Zinc chloride and ammonium thiocyanate together were considered as the inner reagent and mercury (II) chloride was added externally on the top of the gel as an outer reagent. The pH of the solution was maintained at 2.8 for better results [40-41].

2.1.3. Synthesis of cadmium mercury thiocyanate (*CMTC*)

Cadmium mercury thiocyanate single crystal was synthesized using ammonium thiocyanate ($NH_4(SCN)$), mercuric chloride ($HgCl_2$) and cadmium chloride ($CdCl_2$) as precursor materials in de-ionized water [21, 38, 42-43].

$$4NH_4SCN + HgCl_2 + CdCl_2 \rightarrow CdHg(SCN)\downarrow 4NH_4Cl \tag{5}$$

Chemical analysis was carried out for the prepared compound and the measured values were found comparable with the theoretically calculated quantities. Solubility test was carried out for CMTC with various solvents and the solubility of CMTC in water was found to be about 8g/l at 50 ℃ [21]. Also, the solubility was checked with the mixed solvent of acetone-water (4:1) by the gravimetric method at different temperatures. It was observed that 30 ℃ was the optimum temperature for better yield of good quality crystals and the solubility rate increased when the concentration of NaCl or KCl in water-NaCl or water-KCl solvent system increased [42]. By using the temperature lowering method, large single crystals can be harvested from CMTC supersaturated solutions.

2.1.4. Synthesis of diaqua (*thiocyanate*) *manganese mercury-N,N-dimethylacetamide* (*MMTWD*)

Good quality MMTWD complex was synthesized by two-step reaction processes. Manganese Mercury Tetra Thiocyanate (MMTC) was synthesized in the first step using de-ionized water [44].

$$4NH_4SCN + HgCl_2 + \mathrm{MnCl_2} \rightarrow MnHg(SCN)_4 + 4NH_4Cl \tag{6}$$

Inorder to dissolve the co-precipitated NH4Cl, the resultant compound was recrystallized using hot water. Recrystallization of the resultant compound has been done using acetone-water (5:1) mixture for the purpose of the purification. The purified salt was utilized for the further synthesis of MMTWD as per the following reaction scheme.

$$\begin{aligned} &MnHg(SCN)_4 + 2(CH_3)_2 + 2(CH_3)_2N - CO - CH_3 \\ &\rightarrow [MnHg(SCN)_4(H_2O)]\ [(CH_3)_2N - COCH_3]_2 \end{aligned} \tag{7}$$

Precipitated MMTWD was obtained by adding the previously synthesized MMTC to the solution, which was made by the mixture of calculated amounts of Dimethyl Acetamide (DMA) and de-ionized water. This precipitate was recrystallized

twice using water-DMA (1:1) as a mixed solvent. Synthesized product was subjected to CHN analysis for purity test and the results were found to be matching with the theoretical values confirming the formation of desired compound [1, 23-24].

2.1.5. Synthesis of manganese mercury thiocyanate bis-dimethyl sulfoxide (*MMTD*)

Manganese mercury thiocyanate bis-dimethyl sulfoxide was synthesized using ammonium thiocyanate or potassium thiocyanate [26], manganese chloride and mercury chloride as the starting reagents. The solvent used for the synthesis was de-ionized water or double distilled water. In the case of potassium thiocyanate, the chemical reaction will be:

$$4NH_4SCN + MnCl_2 + HgCl_2 \rightarrow MnHg(SCN)_4 + 4NH_4Cl \quad (8)$$

In the case of potassium thiocyanate, the chemical reaction will be

$$4KSCN + MnCl_2 + HgCl_2 \rightarrow MnHg(SCN)_4 + 4KCl \quad (9)$$

As-synthesized MMTC was crushed and the powder was dissolved in mixed solvent of DMSO and de-ionized water. The following chemical reaction describes the process.

$$MnHg(SCN) + 2C_2H_6OS \rightarrow MnHg(SCN)_4(C_2H_6OS)_2 \quad (10)$$

It is reported that good quality crystals were obtained by maintaining the pH of the solution at 3.5 [45] which was varied using hydrochloric acid (HCl) [3, 26]. It is reported that the solubility of the MMTD crystals greatly depend on the pH value and was found to be relatively high at low pH values and decreased with increase in pH values [46].

2.1.6. Synthesis of manganese mercury thiocyanate glycol monomethyl ether (*MMTG*)

In order to synthesize MMTG, MMTC should be synthesized first as described in previous sections. MMTG was synthesized by using Glycol Monomethyl Ether (GME) as a ligand with MMTC in de-ionized water (in volumetric ratio 5:7) [47]. The chemical reaction is as follows;

$$MnHg(SCN) + HO - CH_2 - CH_2 - OCH_3 \rightarrow MnHg(SCN)_4(HO - CH_2 - CH_2 - OCH) \quad (11)$$

Crystalline habits of MMTG are also affected by different pH value of the solution. It was observed that MMTG had very high solubility at low pH value and it decreased rapidly with the increased pH value [29].

2.1.7. Synthesis of zinc manganese thiocyanate (*ZMTC*)

Zinc chloride, manganese chloride, and potassium thiocyanate were used as precursors. The crystal growth was carried out in aqueous solution. The molarity ratio of the precursor material was 1:1:4. The reaction scheme was as follows;

$$ZhCl_2 + MnCl_2 + 4KSCN \rightarrow ZnMn(SCN)_4 + KCL \quad (12)$$

Initially, the output product was in precipitate form and the good quality optical crystals were achieved by successive recrystallization processes [48].

2.1.8. Synthesis of zinc cadmium thiocyanate crystals (*ZCTC*)

ZCTC was synthesized using de-ionized water according to the reaction,

$$ZnX + CdX_2 + 4ASCN \rightarrow ZnCd(SCN)_4 + 4AX \quad (13)$$

where A=K, $NaNH_4$; X=Cl, NO_3, CH_3COO [27]. It was noted that ZCTC possesses very high solubility in water/acetone solution mixture. The crystals were grown by controlled evaporation at 40 ℃ [30] and the quality of the crystal improved by adding HX(X=$ClNO_3CH_3COO$). The solubility studies for ZCTC were carried out with various solvents and it was reported to be about 41 g/l at 50 ℃ [49].

2.1.9. Synthesis of tetrathiourea cadmium tetrathiocyanato zincate (*TCTZ*)

Synthesis of TCTZ follows two folded mechanism as shown in the below chemical reactions. The purest form of ammonium thiocyanate, zinc chloride, cadmium chloride, and thiourea were used as basic reagents [50].

$$4NH_4(SCN) + CdCl_2 + ZnCl_2 \rightarrow ZnCd(SCN)_4 + 4NH_4Cl$$
$$ZnCd(SCN)_4 + 4(CS(NH_2)_2 \rightarrow Zn(SCN)_4Cd(CS(NH_2)_2)_4 \quad (14)$$

The first reaction describes the synthesis of zinc cadmium thiocyanate. The synthesized product was dissolved in hot water and then filtered. The aqueous solution of thiourea was added to the ZCTC complex to form TCTZ compound. The synthesized compound was subjected to recrystallization in order to get pure TCTZ [50]. The single step reaction for the synthesis is as follows;

$$4(N_2H_4CS) + 4(KSCN) + CdCl_2 + ZnCl_2 \rightarrow Cd(N_2H_2CS)_4Zn(SCN)\downarrow + 4KCL \quad (15)$$

The mixed solvent of acetone:water in the ratio 2:1 was used for the crystal growth by the solvent evaporation method.

2.1.10. Synthesis of tetrathiourea mercury tetrathiocynato manganate (*TMTM*)

Synthesis of TMTM follows two-step chemical processes. The analytical grade precursor materials were used for synthesis. The reaction scheme is;

$$MnCl_2 + HgCl_2 + 4KSN \rightarrow MnHg(SCN)_4\downarrow + 4KCL$$
$$MnHg(SCN)_4 + 4(CSN_2H_2) \rightarrow Hg(CSN_2H_4)_4Mn(SCN)_4 \quad (16)$$

Solubility test on TMTM in different solvents was carried out and was found highly soluble in acetone. Very high evaporation and less stability of solution in acetone made the crystal growth difficult in acetone solvent. Therefore it was concluded that water is a better solvent for the growth of TMTM crystals. It was also found that solubility of the material got reduced at higher temperatures and at higher pH values [51-54]. The higher pH values (>5) lead to a decrease in a number of nucleation centers thereby creating needle-like crystals. pH value of 3 was found to be optimum for bulk crystal growth [52].

2.1.11. Synthesis of tetrathiourea mercury tetrathiocynato manganate (*TMTM*)

Synthesis of TMTM follows two-step chemical processes. The analytical grade precursor materials were used for synthesis. The reaction scheme is;

$$MnCl_2 + HgCl_2 + 4KSN \rightarrow MnHg(SCN)_4\downarrow + 4KCL$$
$$MnHg(SCN)_4 + 4(CSN_2H_2) \rightarrow Hg(CSN_2H_4)_4Mn(SCN)_4 \quad (16)$$

Solubility test on TMTM in different solvents was carried out and was found highly soluble in acetone. Very high evaporation and less stability of solution in acetone made the crystal growth difficult in acetone solvent. Therefore it was concluded that water is a better solvent for the growth of TMTM crystals. It was also found that solubility of the material got reduced at higher temperatures and at higher pH values [51-54]. The higher pH values (>5) lead to a decrease in a number of nucleation centers thereby creating needle-like crystals. pH value of 3 was found to be optimum for bulk crystal growth [52].

2.1.12. Synthesis of manganese mercury thiocyanate bis (*N-dimethylformamide*)(*MMTN*)

By using N-dimethylformamide (NMF) as a ligand to the MMTC reactant in de-ionized water, MMTN was synthesized. The chemical reaction can be formulated as shown below:

$$MnHg(SCN)_4 + 2CH_3 - NH - CHO \rightarrow MnHg(SCN)_4(CH_3 - NH - CHO) \quad (17)$$

The preparation of MMTN can also be described by another chemical reaction as follows (where X=Cl, NO3, CH3COO) [55-56];

$$Hg(NO_3)_2 + 4NH_4SCN + MnX_2 + 2H_2O + 2C_2H_5NO \rightarrow MnHg(SCN)_4(C_4H_9NO)_2\downarrow + 4NH_4X \quad (18)$$

2.1.13. Synthesis of Cadmium Mercury Thiocyanate Dimethyl Sulfoxide (*CMTD*)

CMTD were synthesized using Dimethyl Sulfoxide (DMSO) as a ligand to react with CMTC in a mixture of dimethyl sulfoxide and de-ionized water [57-58]. The chemical reaction can be written as follows;

$$CdHg(SCN)_4 + 2(CH_3)_2SO \rightarrow CdHg(SCN)_4 \bullet 2(CH_3)_2SO \quad (19)$$

Solubility studies made for the compound with different solvents showed that the mixture of dimethyl sulphoxide and de-ionized water in the volumetric ratio 3:1 was an optimal one for the growth of good quality crystal [57].

2.1.14. Synthesis of mercury chloride thiocyanate (*MCCTC*)

Appropriate amounts of mercury thiocyanate and cadmium chloride was taken in the molar ratio 3:1 were dissolved in methanol solvent to synthesize MCCTC. The chemical reaction is as follows;

$$3Hg(SCN)_2) + CdCl_2 \rightarrow Hg_3CdCl_2(SCN)_6 \quad (20)$$

The crystal growth of MCCTC was achieved by a saturated solution of MCCTC in the methanol-water mixed solvent in room temperature [59]. After getting the seed crystals, the good quality crystal among them was chosen and used for the bulk single crystal growth [60].

2.1.15. Synthesis of cadmium mercury thiocyanate glycol monomethyl ether (*CMTG*)

Cadmium chloride, mercuric chloride, ammonium thiocyanate and Glycol Monomethyl Ether (GME) were the precursor materials used [61-62]. All the reactions were carried out in an aqueous medium. Initially, CMTC was synthesized as discussed previously. Then the measured volume of GME diluted with de-ionized water was added to CMTC and the supersaturated solution was made. The chemical reaction for the synthesis of CMTG is as follows;

$$CdHg(SCN)_4 + CH_3OC_2H_2O \rightarrow CdHg(SCN)_4(CH_3OC_2H_5O) \quad (21)$$

Crystal growth was achieved by evaporating the resultant solution from the above process. In order to purify the crystals, repeated recrystallization was followed using GME-Water (1:1) as a mixed solvent.

2.1.16. Synthesis of bis (dimethyl sulphoxide) Cadmium Thiocyanate (*DSTC*)

The DSTC preparation was accomplished by the following reaction,

$$Cd(NO_3)_2 \bullet 4H_2O + 2NH_4SCN + 2C_2H_6SO \rightarrow Cd(SCN)_2(C_2H_6SO)_2 + 2NH_4NO_3 + 4H_2O \quad (22)$$

Elemental analysis was carried out to ensure the purity of the product and results were summarized which demonstrate the validity of the chemical composition. Temperature lowering method was employed to grow the single crystal. The preferred pH value for this synthesis was 3. The mixture of water and DMSO in the ratio 3:1 was used as a solvent for the preparation of saturated solution [63].

2.1.17. Synthesis of copper mercury thiocyanate (*CMTC*)

Copper mercury thiocyanate crystals were prepared using potassium thiocyanate, copper chloride,and mercuric chloride as precursor materials. The crystals were synthesized by taking the materials as purchased in stoichiometric ratios and de-ionized water was chosen as a solvent.

$$CuCl_2 + HgCl_2 + 4KSCN \rightarrow CuHg(SCN)_4 + 4CKL \quad (23)$$

Successive filtration and recrystallization were carried out in order to purify the material. A constant temperature of 30℃ was used for growth process [64].

Growing a single crystal from thiocyanate derivatives is challenging. The parameters which affect the crystal growth and its optimization are discussed in detail in Table 1. Among low-temperature crystal growth techniques, slow evaporation solution growth technique is widely followed as it gives well-developed defect free bulk crystals. Growing the organometallic thiocyanate crystals using unidirectional, Shankarnarayan-Ramasamy (SR) method and seed rotation method can be the future scope of this work.

Table 1 Table showing different crystal growth methods, growth time and approximate sizes of the grown crystal

Compound Name	Crystal growth method	Growth Duration (in days)	Harvested crystal size	Ref.
Manganese Mercury Thiocyanate (MMTC)	Slow evaporation method	50 to 60	12×8×6 mm^3	[19]
Cadmium Mercury Thiocyanate (CMTC)	Temperature lowering method, Slow evaporation method	---	18×18×25 mm^3	[42]
Diaqua (thiocyanato) manganese mercury-N, N-dimethylacetamide (MMTWD)	Slow cooling and slow evaporation method	35	1.6×1.3×1.4 cm^3	[24-25]
Manganese Mercury Thiocyanate bis-dimethyl sulfoxide (MMTD)	Slow temperature lowering method	90 to 100	25×18×18 mm^3	[3]
Copper Mercury Thiocyanate (CMTC)	Slow evaporation method	Few weeks	12×8×5 mm^3	[64]
Zinc Cadmium Thiocyanate crystals (ZCTC)	Slow solvent evaporation method	40	5×2×3 mm^3	[65]
Zinc Manganese Thiocyanate (ZMTC)	Gel growth method (Diffusion process in silica gel medium)	30	-----	[48]
Tetrathiourea Cadmium Tetrathiocyanato Zincate (TCTZ)	Slow evaporation method	30	8×1.5×0.5 mm^3	[50]
Tetrathiourea MercuryTetrathiocynato Manganate (TMTM)	Slow evaporation method	40 to 45	-----	[54]
Manganese Mercury Thiocyanate bis (N-methylformamide) (MMTN)	----	----	29×28×14 mm^3	[56]
Cadmium Mercury Thiocyanate Dimethyl sulfoxide (CMTD)	Temperature lowering method	45	25×23×15 mm^3	[57]
Cadmium Mercury Thiocyanate Glycol monomethyl ether (CMTG)	Slow evaporation method	15	10×10×9 mm^3	[61]

3. Results and Discussion

As synthesized bimetallic thiocyanate compounds were subjected to various characterizations viz., single crystal X-ray Diffraction (XRD), linear and non-linear optical studies, Fourier Transform Infrared (FTIR) studies, laser Raman spectral analysis, thermal studies, dielectric studies, etching studies, surface laser damage threshold studies, Vickers micro hardness studies etc. The results which had been published for different compounds are discussed in the following titles.

3.1. Single crystal X-Ray diffraction studies

Singe crystal x-ray diffraction characterization had been carried out for all the bimetallic thiocyanate compounds. The cell parameters and morphology of the compounds were determined. Most commonly, the single crystal XRD was used to determine the parameters like crystal structure, space group, unit cell parameter values, formula unit (z), cell volume (V) and density. Table 2 summarizes all the crystallographic parameters for different thiocyanate compounds which were discussed in the synthesis part. The reported numerical values of the different cell parameters given in Table 2 vary slightly between different syntheses routes for the same compound.

3.2. Fourier transforms infrared spectral analysis

Fourier Transform Infrared (FTIR) spectroscopy is one of the fundamental characterization techniques for finding out the functional groups, coordination of ligand and their bending and stretching vibration modes quantitatively. In this technique, IR radiation is passed through the sample and the resulting molecular absorption and transmission spectrum creating a molecular fingerprint of the sample is recorded. The powdered crystal of various kinds of organometallic

thiocyanate was subjected to FTIR analysis to confirm the presence of functional groups. The spectrum was recorded in the range of 400 to 4000 cm-1.

Table 2 Calculated cell parameters of various bimetallic thiocyanate crystals using single crystal X-Ray diffraction method

Compound Name	Crystal structure	Space group	Unit cell parameter values (Å)	Formula unit (z)	Cell volume $(Å)^3$	Density	Ref.
Manganese mercury-N, N-dimethylacetamide single crystal ($C_{12}H_{22}MnHgN_6O_4S_4$) (MMTWD)	Tetragonal	P4	a=12.2496(4) c=8.0719(6) $\alpha=\beta=\gamma=90^\circ$	2	V=1211.19 (10)	1.916Mg/m^3	[24-25]
Manganese mercury Thiocyanate ($MnHg(SCN)_4$) (MMTC)	Tetragonal	$I\bar{4}$	a=11.3099 c=4.2537 $\alpha=\beta=\gamma=90^\circ$	--	V=547.5	2.959g/cm^3	[19]
Manganese Mercury Thiocyanate bis-dimethyl sulfoxide ($MnHg(SCN)_4(C_2H_6OS)$) (MMTD)	Orthorhombic	$P2_12_12_1$	a=8.6523 b=12.2417 c=15.3705 $\alpha=\beta=\gamma=90^\circ$	4	V=2018.5	2.120g/cm^3	[3]
Manganese mercury Thiocyanate glycol monomethyl ether(MMTG)	Orthorhombic	$Pca2_1$	a=16.2046(16) b=7.2974(5) c=13.5090(14) $\alpha=\beta=\gamma=90^\circ$	4	V=1597.5	2.345Mg/m^3	[29]
Cadmium Mercury Thiocyanate ($CdHg(SCN)_4$) (CMTC)	Tetragonal	$I\bar{4}$	a=11.487(3) c=4.218(1) $\alpha=\beta=\gamma=90^\circ$	2	V=556.6(1)	3.254mg/m^3	[23]
Copper Mercury Thiocyanate ($CuHg(SCN)_4$) (CMTC)	Monoclinic	$I\bar{4}$	a=11.09 b=4.10 c=11.34 $\alpha=\beta=\gamma=90^\circ$	--	V=467	--	[64]
Zinc Cadmium Thiocyanate ($ZnCd(SCN)_4$) (ZCTC)	Tetragonal	$I\bar{4}$	a=11.135(2) c=4.3760(10) $\alpha=\beta=\gamma=90^\circ$	2	V=542.6(2)	2.510 g/cm^3	[65]
Bis Mercury Ferric Chloride Tetra Thiocyanate ($HgFeCl_3(SCN)_4$) (MFCTC)	Monoclinic	$P2_1$	a=16.524 b=8.346 c=6.412	--	V=884.27	--	[66]
Cadmium Mercury Thiocyanate Dimethyl-Sulfoxide ($CdHg(SCN)_4(H_6C_2OS)_2$) (CMTD)	Orthorhombic	$P2_12_12_1$	a=8.5188(6) b=8.5398(7) c=28.224(6)	4	V=2053.3 (5)	2.270g/cm^3	[57]
Tetrathiourea Mercury Tetrathiocyanato Manganite ($C_8H_{16}N_{12}S_8MnHg$) (TMTM)	Tetragonal	$I\bar{4}$	a=b=17.37 c=4.17 $\alpha=\beta=\gamma=90^\circ$	2	V=1257	--	[54]
Manganese Mercury Thiocyanate bis(N-methylformamide) ($MnHg(SCN)_4(C_2H_5NO)_5$) (MMTN)	Orthorhombic	$Pna2_1$	a=16.1203(15) b=7.7373(7) c=15.2135(18)	4	V=1897.5 (3)	2.121g/cm^3	[56]
Mercury Cadmium Chloride Thiocyanate ($Hg_3CdCl_2(SCN)_6$) (MCCTC)	Rhombohedral	R3c	a=11.184 b=11.191 c=59.308	12	V=6493.2	3.47g/cm^3	[59]
Tetrathiourea Cadmium Tetrathiocyanato Zincate ($Zn(SCN)_4Cd(CS(NH_2)_2)_4$) (TCTZ)	Tetragonal	$I\bar{4}$	a=b=17.2334 c=4.2536	--	V=1253.5548	--	[50]
Cadmium Mercury Thiocyanate Glycol monomethyl ether ($CdHg(SCN)_4(CH_3OC_2H_5O)$) (CMTG)	Orthorhombic	$Pca2_1$	a=7.347(2) b=13.436(2) c=16.316(1) $\alpha=\beta=\gamma=90^\circ$	4	V=1610.5	2.523Mg/m^3	[61]
Zinc Mercury Thiocyanate ($ZnHg(SCN)_4$) (ZMTC)	Tetragonal	$I\bar{4}$	a=b=11.032 c=4.429 $\alpha=\beta=\gamma=90^\circ$	----	V=539.03	-----	[41]
Zinc Manganese Thiocyanate ($ZnMn(SCN)_4$) (ZMTC)	Tetragonal	---	a=12.0835 b=12.131 c=8.569 $\alpha=89.91^\circ$; $\beta=90^\circ$; $\gamma=89.99^\circ$	---	V=1256	-----	[48]
Bis(dimethyl sulfoxide) cadmium thiocyanate ($Cd(SCN)_2(DMSO)_2$) (DSTC)	Triclinic	$P\bar{1}$	a=5.9172(15) b=8.0811(12) c=8.1539(12) $\alpha=114.53^\circ$; $\beta=100.91^\circ$; $\gamma=95.44^\circ$	1	V=341.65 (11)	1.870g/cm^3	[63]

Numerous studies show that the CN stretching vibration in FTIR spectrum of Manganese Mercury Thiocyanate (MMTC) often lie above 2100 cm^{-1}, the CS stretching vibration lies between 860-780 cm^{-1} (N-bonding) or 720-690 cm^{-1} (S-bonding) and SCN bending vibration lies near 480 cm^{-1} (N-bonding) or 420 cm^{-1} (S-bonding). A comparative study between the IR frequency bands of MMTC and the absorption peaks of NH_4SCN reveal that the CN stretching of NH_4SCN is shifted from 2075 to 2112 cm^{-1} in MMTC reflecting that the thiocyanate group is coordinated to metal ions through nitrogen and sulfur. Other weak absorption bands observed at 895 and 778 cm^{-1} are attributed to CS stretching of N-bonded and S-bonded complexes respectively [19].

By employing the KBr pellet technique, the FTIR spectrum of Zinc Mercury Thiocyanate (ZMTC) crystal was recorded. The intense peak at 2157.91 and 784.26 cm^{-1} confirms the CN stretching vibration (nCN) and CS stretching respectively. It was reported that the absorption peaks at 445.61 and 469.65 cm^{-1} are due to SCN bending vibrations (dNCS) while those at 892.53 and 938.63 cm^{-1} corresponds to 2dNCS [41].

Tetrathiourea Cadmium Tetrathiocyanato Zincate (TCTZ) was subjected to FTIR spectroscopic characterization and it was reported that in the high-frequency region between 2800 and 3500 cm^{-1}, broad peaks were observed at 3388, 3287 and 3197 cm^{-1} corresponding to asymmetric, bending and symmetric vibrational modes of NH_2 respectively in thiourea molecule. The spectral comparison of pure thiourea and TCTZ confirms the coordination of metal-sulfur bond. The shifting of the peak from 1470 to 1500 cm^{-1}, which is assigned to NCN symmetric stretching vibration of the TCTZ complex in comparison with pure thiourea molecule was observed by the recorded spectrum. The metal-nitrogen bond was confirmed by comparison of CN stretching vibration peak of TCTZ with respect to the pure thiocyanate observed at 2101 and 2063 cm^{-1} respectively. Shifting of C-S stretching frequency from 730 to 706 cm^{-1} confirmed the coordination of metal-sulfur bond [50].

In Manganese Mercury-N, N-dimethylacetamide (MMTWD) the main absorption peaks of MMTC, H_2O, and DMA were observed. Due to the coordination of O atoms with Mn atom, absorption peak assigned for the O-H stretching modes of MMTWD appeared at lower frequencies compared to a pure water molecule. It has been reported that the C-N and C-S stretching modes of MMTWD appear at shifted frequencies compared to MMTC and C=O stretching mode of MMTWD is shifted to a lower frequency compared to the corresponding frequency of DMA [23].

FTIR spectrum of Tetrathiourea Mercury Tetrathiocyanato Manganate (TMTM) was recorded. The main absorption peaks of MMTC and thiourea have been observed in the FTIR spectrum of TMTM. The metal to ligand bonding was confirmed by the shift in wave number observed with respect to the pure thiourea and thiocyanate ion. The metal ion bonding with the sulfur atom of thiourea ligand [$MSC(NH_2)_2$] was confirmed by a shift in C-S symmetric stretching vibration in TMTM from 730 cm^{-1} to a lower frequency of 706 cm^{-1}. It was reported that the intense band at 2079, 810 and 471 cm^{-1} were due to stretching vibration of C-N group of thiocyanate, C-S bonding, and SCN bonding respectively. The standard wave number range for CN stretching vibrational mode, CS stretching mode, and SCN bending modes are 2040-2080 cm^{-1}, 780-860 cm^{-1} and 460-490 cm^{-1} respectively and this range is well compared with the observed data in the recorded spectra. Mn^{2+} and Hg^{2+} are hard and soft electron acceptors, while N(SCN) and S(SCN) are hard and soft electron donors in the structure of MMTC crystal, whereas,in the case of TMTM, the sulfur (thiourea) replaces the place of sulfur (thiocyanate) as the soft electron donor. It is discussed that the formation of three dimensional networks like structure in MMTC is by the distorted tetrahedra HgS_4 and MnN_4 connected by the thiocyanate bridge whereas in TMTM discrete $[Hg(TU)4]^{2+}$ cation and $[Mn(NCS)4]^{2-}$ anion are held together by weak N(TU)-H-S(SCN) hydrogen bond. Interestingly this structural replacement causes the spectral difference between the two compounds [52].

FTIR spectral data were collected for Manganese Mercury Thiocyanate bis-dimethyl sulfoxide (MMTD). The stretching vibration of the C-N bond was observed at 2126 cm^{-1}, which looks shifted to 2212 cm^{-1} when compared with MMTC. The weak and sharp band at 717 cm^{-1} was attributed to C-S stretching. On comparison with DMSO, it was observed that the S-O

vibration frequencies were shifted to lower values. The coordination of O atoms with Mn atom causes weaker bonds between O and S in the coordinated DMSO molecule. The different molecular structure of DMSO in MMTD with respect to the free DMSO was confirmed by the shift in stretching and bending modes of C-H bond, which was attributed to the fact that the DMSO molecule combines with Mn as a monodentate ligand through the O atom [46].

With the motive of qualitatively analyzing the presence of functional group in Mercury Cadmium Chloride Thiocyanate (MCCTC) crystal, the compound crystal was subjected to FTIR and spectrum was recorded. In MCCTC crystal, the CN stretching vibration observed at 2105 cm^{-1} and was found to be shifted towards the lower side when compared to CMTC and MMTC. SCN bending vibrations of MMTC observed at 533 cm^{-1} also shifted to a larger extent in comparison with CMTC (439 and 464 cm^{-1}) and MMTC (447 and 468 cm^{-1}). This leads to the possible distortion in the SCN chromosphere ion caused by the coordination of Hg with Cl, which is the main difference in the bonding of MCCTC when compared to CMTC and MMTC. The existence of Cl in crystal was confirmed by the stretching vibration of Hg-Cl bond by the band at 2824 cm^{-1} [60].

The functional group present in the Zinc-ManganeseThiocyanate Crystal (ZMTC) exhibited characteristic peaks at 673 cm^{-1} and 2347 cm^{-1} representing the stretching vibration of SCN and CN bonds respectively. The band at 1417 cm^{-1} and 1625 cm^{-1} were assigned to symmetric stretching of CN and CS bonds respectively [48].

Prominent absorption peaks of CMTC and DMSO were observed in bis-(dimethyl sulfoxide) Cadmium Mercury Thiocyanate (CMTD). The absorption peak attributed to S-O stretching mode of CMTD was found to be appearing at 1006 cm^{-1} compared to those of pure DMSO at 1050 cm^{-1}. From the spectrum, it was found the CN and CS stretching modes of CMTD appeared at 2106 and 707 cm^{-1} respectively, whereas in CMTC it was observed at 2120 and 773 cm^{-1} respectively. This brought up the difference in the molecular structure of the DMSO in CMTD with a comparison of free DMSO [58]. Fig. 2 shows the FTIR spectrum of ammonium thiocyanate (NH_4SCN) crystal in the region 4000 to 500 cm^{-1} as an example.

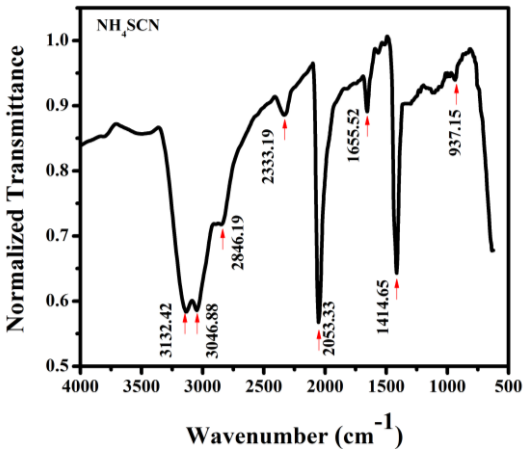

Fig. 2 FTIR spectrum of NH_4SCN

The FTIR spectrum of Cadmium Mercury Thiocyanate Glycol monomethyl ether (CMTG) showed a broad peak at 3488 cm^{-1} arising out of O-H stretching mode. The bending vibrational mode of the hydroxyl group in CMTG crystal was confirmed by the band appearing at 1617 cm^{-1}. The appearance of bands at 2110 cm^{-1} and 1124 cm^{-1} were attributed to C-N and C-O stretching frequency of CMTG respectively. The peaks appearing at 464, 885 and 925 cm^{-1} were reported due to the deformation bending mode of thiocyanate ion (SCN) and its overtone bands. The presence of C-S stretching frequency of CMTG was confirmed by the peak at 716 cm^{-1} [61].

Presence of functional groups, Bis-mercury Ferric Chloride Terathiocyanate (MFCTC) was compared with the major frequency components involved in NH_4SCN. It was reported that the CN stretching frequency observed as strong peaks at 2117 and 2135 cm^{-1} was actually shifted from the stretching frequency (2048.99 cm^{-1}) of free radical thiocyanate ion. As per

Hard Soft Acid Base concept, the coordination of S in SCN with Hg ion was the cause of the shift in frequency and this fact clearly established the incorporation of thiocyanate ligand (SCN) in MFCTC.

The existence of the A-S-C-N-B metal-ligand bandings, where A and B are different metal atoms, was confirmed for the different organometallic thiocyanate crystals using FTIR analysis. Various stretching and bending vibrations of the elements present in each crystal were discussed quantitatively.

3.3. Raman and IR spectral analysis

Raman spectroscopy and Infrared Spectroscopy (IR) are well-known vibration spectroscopic techniques and are always recognized as the complementary spectroscopic techniques. IR spectroscopic bands arise due to changes in dipole moment of the molecule by an electromagnetic wave interaction whereas Raman bands arise from a change in the polarizability of the molecule due to the same interaction. Recent advancement made these two spectroscopic techniques as fundamental analytical tools in materials science. In crystallography, these are sensitive tools which serve for qualitative and quantitative determination of structural incorporated molecule and defects, specification and concentration studies, information about atoms and their bonds, the spatial orientation of dipoles (by IR spectroscopy) and mineral composition studies (by Raman spectroscopy). IR and Raman spectroscopic studies are advantageous because of their non-destructive nature, the requirement of very fewer sample quantities and absence of any sample preparation. Few of the organometallic thiocyanate crystals were also subjected to Raman and IR spectroscopic studies by various crystal growers all around the globe to study the molecular structure of organometallic thiocyanate crystal. Some of these are discussed here.

The Raman and IR spectra of organometallic thiocyanate crystals like ZCTC, CMTC, MMTD, and MMTWD were observed in the spectral range of 100-3000 cm^{-1}. Starting with the IR spectral studies of MMTWD complex crystals, the counterparts of the main absorption peaks of MMTC, H_2O, and DMA in MMTWD can be observed. The coordination of O atom with the Mn atoms and the formation of the hydrogen bonding between H_2O and DMA molecule shifts the absorption peak assigned to the OH stretching mode of MMTWD towards the lower frequency compared with those of H_2O, which causes the weaker bond between O and H in the coordinated H_2O molecules. It was reported that the C-N and C-S stretching modes of MMTWD appears at shifted frequencies compared with those of MMTC, and also C=O stretching mode of MMTWD gets shifted to a lower frequency as compared to the corresponding frequencies of the DMA molecule [24].

Comparative Raman spectral studies of MMTC and MMTWD show that the Raman shifts of the SCN bending and CN stretching modes in MMTWD are somewhat higher compared with those of MMTC [23, 25]. The studies also revealed tell us that the Raman peaks of the SHgS bending and CS stretching modes of MMTWD are higher and lower than those of MMTC respectively. The reason claimed for this is the O(H_2O) coordination with Mn^{2+}. Because the Mn-O bonds are very weak and the bond lengths are much longer than the sum of the single bond covalent radii, there is no peak of Mn-O vibration mode. In a free thiocyanate (SCN^-) ion of NH_4SCN/KSCN, the C-N stretching vibration appears comparatively lower than that of coordinated SCN ion. This confirms the coordination of thiocyanate in MMTWD. The electron transformation model explains this coordination mechanism. For example, in the complex of MMTWD, the metal ion of Mn^{2+} and Hg^{2+} behaves as an electron acceptor and the ligands of thiocyanate (SCN^-) ion and dimethylacetamide acts as an electron donor. Thus the electron transformation forms the bonding/coordination [1]. Fig. 3 depicts the Raman and IR spectra of MMTWD single crystal [24].

The IR transmission spectrum and the spectral data of MMTD in comparison with MMTC and DMSO give the information that the absorption peaks assigned to S-O stretching modes of MMTD appear at a lower frequency compared with DMSO peaks with coordination of O atom with Mn atom being the reason for this. This leads to a weaker bond between O and S in the coordination of the DMSO molecule. The shifted frequencies of C-N and C-S stretching modes of

MMTD were also justified with the same reason. By these observations from IR spectral studies of MMTD, it was concluded that the molecular structure of DMSO in MMTD differs from that of the free DMSO [3].

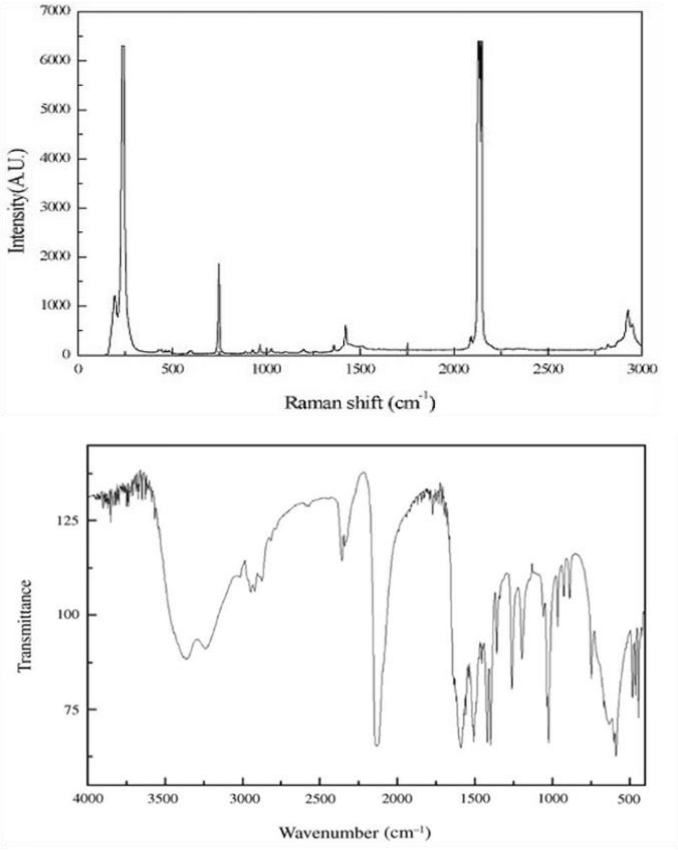

Fig. 3 Raman and IR spectra of MMTWD [1, 24]

ZCTC single crystal was subjected to IR spectral analysis and the spectral data gives the information that nCN often lies higher than nCS and dSCN. The nCS and dSCN againsplit as S-bonding and N-bonding. By the IR spectroscopic studies of ZCTC, the metal-nitrogen and the metal-sulfur coordination in their structures were confirmed [67-68].

CMTC crystal was subjected to laser Raman spectroscopy in the spectral range of 0 to 4000 cm^{-1}. The studies confirmed the presence of S-Hg-S and N-Cd-N bending vibrations. The different peaks appearing across the Raman shift confirm the bending mode of NCS, C=S stretching frequency and C-N stretching vibration. As explained by the electron transformation mode, the Raman shifts of C=N stretching mode in the CMTC crystals were greater than those in free thiocyanate [58].

3.4. Thermal analysis

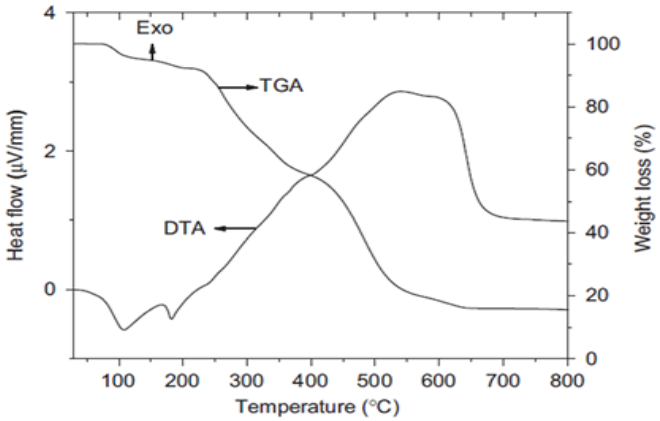

Fig. 4 TG-DTA trace of MMTWD [23]

Table 3 Thermo-analytical data of different organometallic thiocyanate crystals

Compounds	Percentage of weight loss		TGA Temp. range (℃)	Species lost	DTA/DSC Peak Temp. (℃)	Color of residue	Weight percentage of the end product		Ref.
	Calc.	Obs.					Calc.	Obs.	
Manganese mercury-N, N-dimethylacetamide single crystal (MMTWD)	5.16	5.09	90 to 110	Two coordinated water molecules	9.9(endo), 97.7(endo), 139.9(endo), 181.3(endo), 235.8(endo), 258.6(endo), 349.9(endo), 403.9(endo), 529.7(endo).	Gray	12.45	12.45	[24] [25]
	24.92	24.62	110 to 240	Two DMA molecules					
	--	--	Above 240	HgS, MnS, Carbon disulfide, Cyanogenand Nitrogen					
Manganese Mercury Thiocyanate (MMTC)	26.39	26.81	288.86 to 429.74	$-3/2(CN)_2 - 1/2N_2 - 1/2CS_2$	371.4(endo), 383.8(exo), 545.1(endo), 704.2(endo).	Gray	--	28.67	[19]
	55.45	53.63	429.74 to 725.84	$-1/2CS_2 - HgS$					
Manganese Mercury Thiocyanate bis-dimethyl sulfoxide (MMTD)	24.22	24.88	Above 145	Two coordinate DMSO	--	Gray	13.57	13.81	[3]
Manganese mercury Thiocyanate glycol monomethyl ether (MMTG)	13.475	13.856	145 to 296.97	Coordinator-GME ($HO-CH_2-CH_2-OCH_3$) Molecule	--	Gray	14.98	15.49	[29]
Copper Mercury Thiocyanate (CMTC)	No loss percentage of species were mentioned in literature		300	--	253.8(endo) 771.4(endo)	--	--	--	[64]
Cadmium Mercury Thiocyanate (CMTC)	30.83	30.31	197.9 to 432.4	2C($2CO_2$), 2S(SO_2), and 4N($2N_2$)	266.7(exo) 329.8(exo) 450.9(exo) 583.2(endo)	--	--	--	[42]
	42.68	42.65	432.4to 947.6	Hgs					
	2.94	2.93	947.6 to 1100	Oxidation Preocess					
Bis(dimethyl sulfoxide) cadmium thiocyanate (DSTC)	40.6	41.1	134 to 290	Two coordinate DMSO	169(endo) 320(exo) 470(exo)	Gray	--	--	[63]
	21.9	21.2	290 to 610	$1/2CS_2$, $3/4(CN)_2$, $1/4N_2$					
Zinc Cadmium Thiocyanate (ZCTC)	4.75	4.32	234.20 to 336.80	-3/8($CN)_2$	374.4(endo) 420.8(exo) 762(endo)	--	--	--	[65]
	26.95	26.71	336.80 to 652.81	-9/8($CN)_2$-1/2N_2-1/2CS_2					
Bis Mercury Ferric Chloride Tetra Thiocyanate (MFCTC)	--	--	234.31	FeS, HgS, CS_2, $(CN)_2$, Cl and N	234.31(exo) 231.57(endo)	--	--	--	[66]
	64	64.8	288.1 to 509.99						
Cadmium Mercury Thiocyanate Dimethyl-Sulfoxide (CMTD	--	22.33%	150 to 270	2 coordinated DMSO	150(endo) 219(endo)	--	--	20.13	[57]
		--	273 to 841	N_2, CN_2, CS_2, CdS and HgS					
Mercury Tetrathiocyanato Manganate (TMTM)	39	37.95	205 to 237	Four thiourea molecules from the complex. Finally corresponding metal, CS_2, N_2, $(CN)_2$	--	--	10.98	11.18	[54]
Manganese Mercury Thiocyanate bis (N-methylformamide) (MMTN)	--	2.10	162.7 to 210	Breakdown of three SCN Structure	202.8(exo) 403.1^{0}C(exo) 491.1(Endo) 600.4(exo) 828.5(endo) 914.9(exo) 1362.9(exo)	Gray	12.6	15.48	[56]
	--	28.34	Above 210	CO_2, CO, SO_2, N_2					
	--	50.28	Above 491.1	HgS, carbon, $MnHg_{1-x}S_{2-x}$, Formation of MnS					
Tetrathiourea Cadmium Tetrathiocyanato Zincate (TCTZ)	--	--	200 to 400	Four thiourea molecules with N_2, CN_2, CS_2	163(endo)	--	27.34	27.13	[50]
Cadmium Mercury Thiocyanate Glycol monomethyl ether (CMTG)	--	5.146	Above 155	Glycol monomethyl ether (GME)	115(endo)	--	--	--	[61]
				N_2, CN_2, CS_2, CdS					
Zinc Mercury Thiocyanate (ZMTC)	--	49.25	310 to 405	Half CS_2 and Sublimation of Hg	405(exo)	Yellowish White	--	26.13	[41]
	--	24.62	405 to 600	CS_2, ½ $(CN)_2$, 3/4N_2					
Zinc Manganese Thiocyanate (ZMTC)	--	--	800 to 1168	--	806(endo)	--	--	--	[48]

Thermal decomposition studies are common for the crystals which have been used in real time applications. There are different quantitative as well as qualitative techniques for thermal decomposition studies of materials. The plots which are

produced by these kinds of characterizations are known as thermograms. Fig. 4 depicts a sample thermogram of MMTWD single crystal [23]. Thermal analysis of different kinds like thermogravimetric, differential scanning calorimetry and differential thermal analysis were carried out in various conditions for all the bimetallic thiocyanate compounds. Table 3 summarizes the data collected from thermal analysis characterization for different compounds.

Thermogravimetric and differential thermal analysis of Manganese mercury-N, N-dimethylacetamide single crystal (MMTWD) sample were carried out from room temperature to 1000℃ in a nitrogen atmosphere at a heating rate of 20℃/min. TGA studies reveal that MMTWD is thermally stable up to 90 ℃, after which the sample undergoes decomposition. The chemical reaction of thermal decomposition (under nitrogen flux) may be described by the following process [1, 23-24].

$$\begin{aligned} &MnHg(SCN)_4(H_2O)\bullet 2C_4H_9NO \rightarrow MnHg(SCN)_4(C_4H_9NO)_2 + 2H_2O\uparrow \\ &MnHg(SCN)_2(C_4H_9NO)_2 \rightarrow MnHg(SCN)_4 + 2C_4H_9NO\uparrow \\ &MnHgS_2 \rightarrow MnHg_{1-x}S_{2-x} +_x HgS\uparrow \\ &MnHg_{1-x}S_{2-x} \rightarrow MnS + (1-x)HgS\uparrow \end{aligned} \tag{24}$$

From the decomposition data of MMTWD, it was concluded that the crystal possesses good thermal stability and does not show any hygroscopic and efflorescent effect for a long time.

Thermal studies of Manganese Mercury Thiocyanate bis-dimethyl sulfoxide (MMTD) were carried out from room temperature to 760 ℃. Beyond 145 ℃, sample started to decompose. The percentage of lost species at this temperature was 24.88% which was comparable to the theoretical value (24.22%). From this, it was concluded that there are two dimethyl sulfoxide (DMSO) molecules in MMTD molecule [3, 26, 45].

In case of Manganese Mercury Thiocyanate (MMTC), the decomposition of the compound started at 289 ℃ indicating the higher thermal stability of MMTC. The following chemical equation shows the step by step thermal decomposition of the material.

$$MnHg(SCN)_4 \rightarrow Mn(SCN)_2 + Hg(SCN)_2 \rightarrow MnS + HgS + Cs_2 + \frac{1}{2}N_2 + \frac{2}{3}(CN)_2 \tag{25}$$

The DTA resulted in three endothermic and one exothermic peak due to the breakdown of three-dimensional steric structure, the elimination of gases and the sublimation of HgS [2].

Manganese Mercury Thiocyanate Glycol monomethyl ether (MMTG) was subjected to thermal analysis and it was found that there was no phase change from room temperature to 145 ℃ but it decomposed above this temperature. The percentage of lost species for different temperature level was tabulated. The DTA reveals several endothermic or exothermic peaks due to the decomposition and elimination of the volatile compounds [29]. The color of the pyrolysis product was gray, whose percentage of 15.496% was close to that of the theoretical value (14.980%).

At normal temperature and pressure, bis(dimethyl sulfoxide) cadmium thiocyanate (DSTC) crystal possess good stability and do not show any hygroscopic and efflorescent effect for a long time. The TGA and DSC studies of DSTC revealed that the thermal decomposition started at 134 ℃ and proceeded in two steps. The following equations describe the decompositions of DSTC crystal [63].

$$\begin{aligned} &Cd(SCN)_2(DMSO)_2 \rightarrow Cd(SCN)_2 + 2DMSO\uparrow \\ &Cd(SCN)_2 \rightarrow CdS + \frac{1}{2}CS_2\uparrow + \frac{4}{3}(CN)_2\uparrow + \frac{1}{4}N_2\uparrow \end{aligned} \tag{26}$$

The combined thermogravimetric and differential thermal analysis of Copper Mercury Thiocyanate (CMTC) crystal was carried out from room temperature to 1100 ℃ under a nitrogen atmosphere with a heating rate 20 ℃. The crystal

possessed single stage weight loss at 300 ℃ and no weight loss was observed below this temperature. DTA data showed two endothermic peaks at 253.8 ℃ and 771.4 ℃ corresponding to decomposition of the CMTC compound [64].

In the atmosphere of nitrogen, TG/DTA was carried out for Zinc Mercury Thiocyanate (ZMTC) crystal in the range 500-600 ℃. It was observed that zinc mercury thiocyanate crystal was thermally stable up to 310 ℃. The decomposition data are given in Table 3. The DTA resulted in an exothermic peak at 405 ℃ corresponding to the evolution of volatile gases [41].

The thermal stability of zinc manganese thiocyanate had been tested by TG/DTA by heating until 1200 ℃ at a heating rate of 10 ℃ per minute under a nitrogen atmosphere. It was reported that zinc manganese thiocyanate crystal was thermally stable up to 800 ℃ and a single stage weight loss occurred in the temperature range of 800 ℃ to 1168 ℃. Sharp endothermic peak at 806 ℃ was observed in DTA analysis [48].

It was mentioned that Zinc Cadmium Thiocyanate (ZCTC) was thermally stable up to 350 ℃. Interestingly TGA results show a slight weight gain at 274 ℃ illustrating the possibility of absorption of nitrogen by the crystal [27].

Bi'sMercury Ferric Chloride Tetra Thiocyanate (MFCTC) was subjected to TG/DTA and DSC measurements in the temperature range of 28-1200 ℃ and 30-330 ℃ respectively. From DTA trace, it was observed that the first decomposition occurs at about 234.3 ℃, which was also evidenced from the DSC peak observed at ~ 231.6 ℃. The species escaped at a different temperature during the experiment is tabulated. It could be noticed that the thermal stability of MFCTC (234.31 ℃) was superior to the material of the same family [66].

Thermal analysis and physiochemical changes of TetrathioureaMercury TetrathiocyanatoManganate (TMTM) were studied by TG/DTA. The analysiswas carried out from room temperature to 1000 ℃ in the nitrogen atmosphere at the heating rate of 20 ℃ per min. TGA revealed that the compound was thermally stable upto 205 ℃ beyond which there was an appreciable weight loss. The percentages of weight loss at different temperatures are tabulated. The final residue was MnS (11.18%) which agreed well with the theoretical value of MnS 11.18% [52].

Manganese Mercury Thiocyanate bis(N-dimethylformamide) (MMTN) crystals were subjected to TGA and DTA analysis. The decomposition reaction reported in the literature [56] is as follows.

$$
\begin{aligned}
&8MnHg(SCN)_4(C_2H_5NO)_2 + (8y - 4x - xy + 60)O \rightarrow \\
&8MnHgS_2 + 8XC + 2y(8-x)CO_2 + 2(4-y)(8-x)CO + 16SO_2 + 40H_2O + 24N_2 \\
&MnHg(SCN)_4(C_2H_5NO)_2 \rightarrow MnHg(SCN)_4 + (C_2H_5NO)_2 \\
&MnHg(SCN)_4 + (6-x)O_2 \rightarrow MnHgS_2 + 2xCO_2 + 2(4-x)CO + 2SO_2 + 2N_2 \\
&MnHgS_2 \rightarrow MnHg_{(1-x)}S_{(2-x)} + xHgS \rightarrow MnS + HgS \\
&(x+2y)C = (x+y)O_2 \rightarrow xCO_2 + 2yCO \\
&MnS + 2O_2 \rightarrow MnSO_4 \\
&4MnS + 7O_2 \rightarrow 2Mn_2O_3 + 4SO_2 \\
&2MnSO_2 + O_2 \rightarrow 2Mn_2O_3 + 2SO_2 \\
&6M_2O_3 \rightarrow 4Mn_3O_4 + O_2
\end{aligned}
\tag{27}
$$

The other decomposition data are given in Table 3.

The thermal stability of Mercury Cadmium Chloride Thiocyanate (MCCTC) was studied in the temperature range of 40 to 481 ℃ at the scanning rate of 20 K/min in a nitrogen atmosphere. Three major decomposition temperatures at ~ 172.8 ℃, 211 ℃ and ~ 220.6 ℃ were reported [60]. The DTA analysis revealed two exothermic peaks around 192.3 ℃ and 270.4 ℃.

Cadmium Mercury Thiocyanate (CMTC) single crystal was characterized by TG/DTA and it is reported that the decomposition of the compound starts from 197.9 ℃. The other decomposition data with respect to different temperature ranges are collected and given in Table 3 [43].

Thermal stability and physiochemical changes of Cadmium Mercury Thiocyanate bis (dimethyl sulfoxide) (CMTD) were studied by TG/DTA and DSC. The temperature range used for the study was from room temperature to 1000 ℃ in a nitrogen atmosphere at a heating rate of 20 ℃ per minute. From the data of TG/TDA analysis, it was revealed that the CMTD compound was thermally stable up to 150 ℃ [58].

The TG/DTA studies of Cadmium Mercury Thiocyanate Glycol monomethyl ether (CMTG) reveal that the compound was thermally stable upto 115 ℃. Interestingly the surface of the CMTG crystal readily reacts with atmosphere and formed a white powdery layer on the surface which led to the conclusion that the atmospheric stability of the CMTG crystal was relatively low [61].

Review on thermal stability of different organometallic thiocyanate crystal concludes the following points;

- The zinc manganese thiocyanate crystal is thermally stable up to 800 ℃ which is highest among all the organometallic thiocyanate crystals [48].
- Zinc cadmium thiocyanate, zinc mercury thiocyanate,and manganese mercury thiocyanate are the other few organometallic thiocyanate crystals which exhibit considerable thermal stability [2, 27, 41].

3.5. Microhardness studies

Hardness is defined as the resistance to indentation and can be determined by measuring the permanent depth of the indentation. In general, the hardness is always claimed as a characteristic property of the material and not as a fundamental physical property. The hardness of the material to deformation is evaluated and this test can be performed on a macroscopic or microscopic scale. For a fixed force and a given indenter, the indentation and the hardness of the material are inversely proportional. The resistance of a material to plastic deformation can be quantified by hardness test. Since hardness is an arbitrary quantity rather than the fundamental material property it gives only a comparative idea of the material's resistance to plastic deformation. Therefore different hardness techniques have different scales [69].

Recognizing and reducing the errors in the indentation test is also an important issue and the most common source of error encountered is the strain hardening effect of the process. However, the effect can be minimized with a smaller indentation which has been experimentally determined through "strainless hardness test".

If the indentation is large compared to surface roughness, the surface finish,and the indenter do not create any errors on the hardness measurement. This is useful while measuring the hardness of the practical surface. The indentation left after the load is removed is known as "recover" or more precisely as "swallowing".

The indentation of spherical indenters is stayed symmetrical and spherical with a large radius. So for very hard materials, the radius can be three times larger than the indenter's radius and the effect is attributed to the release of elastic stress. This effect may lead to some errors in the diameter and depth of the indentation. The point to be noted in this scenario is the error from the change in diameter is only a few percents when compared to the error from the depth change.

The routinely used term in literature to describe the hardness testing of materials with low applied loads is micro-hardness, in particular as micro-indentation hardness test. Mechanical properties of small scale sample like a thin film and small objects cannot be measured by the conventional method of hardness testing. In such circumstances indenting a material with an impression is done to determine such properties. Micro-indentation tests typically use force less than 2N. In this testing, a diamond indenter of specific geometry with a known applied force of 1 to 1000 of is impressed onto the sample surface. Because of its perfection, one can observe the change in hardness in terms of microscopic scale. Polishing of the sample surface is required in both the test methods to achieve accurate results.

The two commonly used micro-hardness tests are "Vickers hardness test (H_V)" and "Knoop hardness test (H_K)". In the Vickers test, both the diagonals of the sample are measured and the average value can be used to calculate the Vickers

pyramid number. In the Knoop test, only the largest diagonal is measured and the Knoop hardness number is computed based on the ratio of applied force to the surface area of the indent itself. Both the quantities have a unit in term of Kgf/mm2.

The Vickers micro-hardness test is a widely used technique for hardness measurements in the literature of organometallic thiocyanate crystals. For the load below 1Kgf, the Vickers hardness (H_V) is calculated using the equation,

$$Hv = 1.8544 * \frac{L}{d^2} (Kg / mm^2) \tag{28}$$

where L is the load in gram force and d is the mean of two diagonals in millimeters.

In order to utilize the grown crystals in making of any device, the studies regarding its mechanical strength play a vital role. The structure and molecular composition of crystals greatly influence mechanical properties. Micro-hardness measurements were carried out on various organometallic thiocyanate crystals with pyramidal diamond indenter by varying the applied loads from 5 to 30 g for an indenter time of 10 s at room temperature and reported the same [14-15, 36, 40, 44]. Vickers micro-hardness number was calculated using the equation $H_V=1.8544L/d^2$ Kg/mm^2 with L as the applied load in Kg and d as the average diagonal length of the indentation mark in mm.

Fig. 5 is an example graph of the variation of micro-hardness with the applied load for MMTC and MMTD crystals. It was dominantly observed that the micro-hardness number increases with increasing load in all the cases of organometallic thiocyanate complexes.

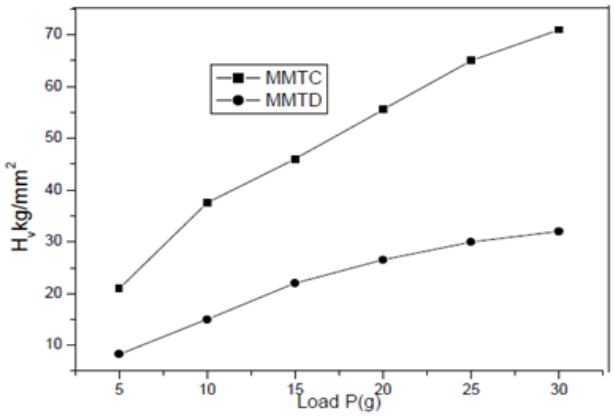

Fig. 5 Variation of Vickers hardness number with load [26]

The calculated Vickers number for different thiocyanate crystals and its comparison with other well known organometallic NLO crystals are summarized in Table 4.

Table 4 Meyer's index number and Vicker's hardness numbers for different organometallic thiocyanate crystals

Compound Name	Vicker's Hardness Number (VHN) in Kg/mm^2	VHN of other well known organic NLO crystals (for comparison) in Kg/mm^2	Mayer's index number	Reference
MMTC	71.4	Urea=6.5to11; N-methyl urea=12to19; CMTD=47; ZTS=116	6.07	[19]
MMTD	32.5	ZCTC=116;BTCC=136;CTA=81	7.2	[46]
TMTM	---	---	3.07	[52]
MCCTC	---	---	1.73	[60]
CMTC	---	---	2.04	[70]

In a fewkinds of literature, Meyer's index number "n" was also calculated using Meyer's law, which relates the load and indentation diagonal length as;

$$P = kd^n \tag{29}$$

$$\log p = \log k + n \log d \tag{30}$$

where *k* is the material constant and *n* is Meyer's index [19]. A graph plotted for *log p* against *log d* gives a straight line and could be used to calculate Meyer's index value "*n*". The slope of the straight line gives the value of the work hardening coefficient "*n*". The calculated Meyer's index for different thiocyanate complexes is also given in Table 4.

A point to be noted here is, HV should increase with the increase in p if n>2 and decrease if n<2. Harder and the softer materials are distinguished based on the value of n and if n lies between 1 and 1.6 the materials are considered to be harder materials and above 1.6 are softer materials.

The calculated Vickers number for different thiocyanate crystals and its comparison with other well known organometallic NLO crystals are summarized in Table 4.

3.6. Linear optical and second order nonlinear optical studies

The presence of delocalized π-electron systems, connecting donor and acceptor groups, which enhance the asymmetric polarizability of NLO materials, causes the macroscopic origin of nonlinearity in it. Each type of constituent chemical bond that has contributions to the total nonlinearity in the material is regarded as one part of the whole crystal. The distribution of valence electrons of the metallic elements is an important factor that strongly affects the linear and nonlinear properties of each type of constituent chemical bond [22].

NLO property of materials could be evaluated from second harmonic generation efficiency test that can be performed by the Kurtz and Perry powder technique using Q-switched, mode-locked Nd-YAG laser operating at the fundamental wavelength 1064 nm. Various laser powers ranging from 2.1 to 6.2 mJ/pulse were reported for such experiments [3, 19, 42, 71]. The experimental setup used a mirror and 50:50 beam splitter to generate a beam with a pulse energy in this range. The laser can be operated in two modes namely single and multi-shot modes. In the single shot mode, the laser emits a single 8 ns pulse and in case of multi-shot mode, the laser produces a continuous train of 8 ns laser pulses at a repetition rate of 10 Hz in 900 geometry [23]. The fundamental beam was filtered and passed through an infrared filter and then made to fall on the microcrystalline powdered sample packed in a micro-capillary tube of the uniform bore. The light emitted by the sample was detected by a photodiode detector and oscilloscope assembly. For the Second Harmonic Generation (SHG) efficiency measurements, most likely microcrystalline materials like urea and KDP were used as reference samples. When a laser input from 2.1 to 6.2 mJ/pulse power was passed through the sample, a second harmonic signal of different wavelengths gets produced which was compared with the reference material to calculate the second harmonic generation efficiency of the sample of interest.

Consider,for example, an organometallic thiocyanate complex like MMTC. When a laser input of 6.2 mJ was passed through an organometallic thiocyanate complex like MMTC, the second harmonic signal of 532 nm was produced and the experimental data confirmed a Second Harmonic (SHG) efficiency of nearly 18 times that of urea [19]. Thus, the second harmonic generation efficiency of MMTC was found to be very much higher than that of other members like CMTC, CMTD, and BTCC of the organometallic family as well as the conventional laser materials like KDP, LAP,and BBO (Potassium Dihydrogen Phosphate, L-arginine phosphate, Beta Barium Borate). It was also examined and reported that La^{3+} and Na^{3+} doped MMTC crystals were having SHG efficiency of nearly 19.53 and 20.02 times higher than that of Urea. These results proved that the increase of SHG efficiency of pure MMTC in presence of dopants [39].

The second harmonic generation tests were carried out by Kurtz-Perry powder method for all the organometallic thiocyanate crystals and the results are tabulated in Table 5.

Since single crystals are mainly used in optical applications, the optical transmission range and the transparency cutoff are important. The optical absorption spectra of MMTC single crystal were recorded in the range of 200-2500 nm. It can be observed from the spectra that MMTC has a larger transmission window lying in the range of 373-2250 nm without any absorption peak. The UV cutoff wavelength of MMTC occurs at 373 nm, which is nearly the same as that of CMTC. This

transparent nature in the UV-Vis-NIR region can be exploited for various NLO applications. The transparency percentage of MMTC at standard violet light of 404 nm is 27.36%, which is lower than that of CMTC, whose transparent percentage at this wavelength is 50%. As a candidate material for the generation of blue-violet light using a diode laser, MMTC is inferior to CMTC [2, 19].

Table 5 A comparison of SHG efficiency and fundamental UV cut-off wavelength of organometallic thiocyanate crystals

Crystal	UV-Vis cut-offwavelength (nm)	SHG Efficiency	Ref.
Manganese mercury-N, N-dimethylacetamide single crystal (MMTWD)	360	4 times MMTWMP	[24-25]
Manganese mercury Thiocyanate (MMTC)	373	18 times Urea	[19]
Manganese Mercury Thiocyanate bis-dimethyl sulfoxide (MMTD)	375	24.8 times Urea	[3]
Manganese Mercury Thiocyanate Glycol monomethyl ether (MMTG)	375	Nearly to Urea	[29]
Cadmium Mercury Thiocyanate (CMTC)	372	11.3 times Urea	[42]
Copper Mercury Thiocyanate (CMTC)	390	0.1 times KDP	[64]
Zinc Cadmium Thiocyanate (ZCTC)	290	12 times Urea	[65]
Cadmium Mercury Thiocyanate Dimethyl-Sulfoxide (CMTD)	360	1.13 times Urea 6.5 times of KDP	[57]
Tetrathiourea Mercury Tetrathiocyanato Manganate (TMTM)	350	10 times KDP	[54]
Manganese Mercury Thiocyanate bis (N-methylformamide) (MMTN)	354	0.9 times Urea	[56]
Mercury Cadmium Chloride Thiocyanate (MCCTC)	300	17 times KDP	[60]
Tetrathiourea Cadmium Tetrathiocyanato Zincate (TCTZ)	290	2.79 times KDP 0.4 times Urea	[50]
Cadmium Mercury Thiocyanate Glycol monomethyl ether (CMTG)	366	5 times Urea 26 times KDP	[61]
Zinc Mercury Thiocyanate (ZMTC)	260	14 times Urea	[41]
Zinc Manganese Thiocyanate (ZMTC)	380	--	[48]

The optical absorption spectra of MMTWD lie in the range of 360-1970 nm. The UV transparency cutoff of MMTWD crystal occurs at 360 nm, while that of MMTC and MMTD at 373 and 375 nm, respectively. The optical transmission at standard violet light of 404 nm was found to be 55.17%, which was higher than that of MMTC and MMTD, whose transmissions at this wavelength are 44.81% and 27.36%, respectively. Interestingly MMTWD showed nearly 94% of transparency in the entire visible region. However, the intensities of the detected second harmonic signals of MMTWD are smaller than that of MMTC and MMTD, but it was concluded that the MMTWD is an effective crystal for NLO applications [1, 23].

The transmission spectra of MMTD crystals lie in 375-2560 nm range. The UV transparency cutoff wavelength of MMTD was 375 nm and the optical transmission of MMTD for standard violet light (at the wavelength of 404 nm) was found 44.81%, which was 17.45% higher than that of MMTC. Therefore, MMTD was found to be superior to MMTC as a candidate material for the generation of blue-violet light using a diode laser [3, 45].

The optical transmission spectrum of copper mercury thiocyanate crystal was measured in the range of 300-2000 nm. The UV transparency cutoff wavelength of CMTC was reported to be at 390 nm and the sample was found to be transparent in the range of 390-973 nm concluding that CMTC has the good optical transmission in the entire visible region [64].

From the transmission spectra of an MMTG crystal, it was reported that the transparency region lies in the range of 375-2265 nm. The UV transparency cutoff of MMTG crystal occurs at 375 nm and the transparency percentage at standard violet light with the wavelength of 404 nm was calculated to be 33.54%, which was higher than that of MMTC [29].

The optical transmission spectrum of CMTC single crystal was recorded in the range 190-1100 nm. The CMTC single crystal showed maximum transparency of 60% in the entire region with UV cut-off wavelength of 372 nm [42].

The UV cut-off wavelength of ZCTC occurred at 290 nm. It is well known that efficient NLO crystal has optical transparency at a lower cut-off wavelength between 200 and 400 nm. In the entire visible region, the optical absorption spectrum was flat and constant in case of ZCTC. For transmission normal to (100) plane, the average transmittance of 70% in the spectra between 330 and 2280 nm was found with transparency percentages of 74.16% and 73.22% at standard violet light of 404 and 380 nm respectively, which are much higher than that of CMTC [65, 68].

The UV-Vis-NIR study of the Zinc Mercury Thiocyanate Crystal (ZMTC) was performed. It was reported that the UV transmission spectra were taken for the solution of copper doped ZMTC crystal, prepared using the solvent of the ethanol-water mixture in 1:1 ratio. Obtained crystal size was not sufficient to perform optical transmission studies in crystal form and hence was dissolved in liquid for measurements. The transparency cut off occurred at 260 nm and the transparency wavelength range was fairly smooth compared to pure ZMTC [41]. The optical behavior of zinc manganese thiocyanate (ZMTC) was measured in the wavelength range of 200-2000 nm. From the recorded measurement, the crystal was observed to be transparent in the wavelength range 390-1193 nm with UV cut-off occurring at 380 nm which was nearly equal to MMTD crystal [48].

The absorption spectrum of the TetrathioureaCadmium TetrathiocyanatoZincate (TCTZ) single crystal was recorded in the range of 200-1100 nm. The thickness of the sample used for the measurement was 1 mm. The cutoff wavelength for TCTZ was observed at 290 nm which was low compared to CMTC (381 nm), MMTC (373 nm) and adducts of bimetallic thiocyanate single crystals. No absorption was found in the entire UV and visible region. This show that TCTZ single crystal could be a suitable material for the generation of blue-violet light [50].

The optical absorption spectrum of MFCTC (bis mercury ferric chloride tetra thiocyanate) crystal was recorded in the range 200-1200 nm. Fig. 6 shows the UV-Vis-NIR spectrum for MFCTC single crystal [66]. The spectrum revealed that the UV cutoff wavelength occurred at about 338 nm. Beyond the cutoff wavelength, the sample exhibits very less absorption (0.02) in the entire visible and IR (up to 1200 nm) region. Hence, it is concluded that the sample possesses broad optical transparency from 338 nm to 1200 nm. However, the Fe^{3+} ion leads to the dark brown color in appearance, which is the drawback for NLO material as far as the optical transparency is concerned [66].

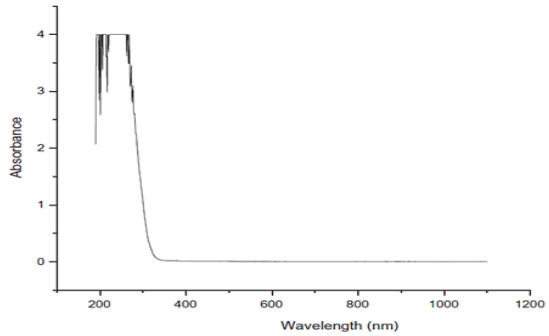

Fig. 6 UV-Vis-NIR absorption spectrum of MFCTC [66]

The optical transmission spectrum of TMTM (tetrathiourea mercury tetrathiocyanato manganate) crystal was recorded in the wavelength range of 200-2000 nm. The optical transmission spectrum of TMTM single crystal showed a UV cutoff wavelength to be around 350 nm. The absorption peaks observed in the visible region might be due to the presence of Mn^{2+} ion in the resulting compound. Various bands in the NIR region are attributed to the overtones and their combinations [53].

The transparent region of MMTN (manganese mercury thiocyanate bis(N-methylformamide)) crystal lies in the range of 354-1506 nm. The UV transparency cut off of MMTN crystal occurs at 354 nm which is comparable with MMTC [56].

MCCTC (mercury cadmium chloride thiocyanate) crystal with suitable thickness was used to record the optical transmission spectrum in the range from 200 to 2500 nm. The optical studies of MCCTC concluded that the percentage of

transmission was very high in the entire UV to IR region without any abnormal peak and the cutoff wavelength was around 300 nm. Among the analogs of thiocyanate reported so far, MCCTC has the wide optical window between 300 and 2500 nm and its lower cutoff wavelength was lesser than that of CMTC (370 nm) and MMTC (373 nm). This shows the suitability of the crystal for nonlinear optical and photonic applications [60].

The transmittance spectrum of CMTG (cadmium mercury tetrathiocyanate (glycol monomethyl ether)) single crystal showed maximum transparency of 56% and UV cutoff wavelength of 366 nm was observed for the CMTG single crystals [61].

The optical transmission spectrum of CMTD (cadmium mercury thiocyanate dimethyl sulphoxide) single crystal was recorded in the range 190-1100 nm. The CMTD single crystal grown at the pH value of 3.5 shows maximum transparency (75%) in the entire visible region compared with crystals grown at other pH values. UV cutoff wavelength of CMTD was found to be 360 nm. It showed a violet shift at 15 and 18 nm compared to bis-(dimethyl sulfoxide) Manganese Mercury Thiocyanate (MMTD) and CMTC crystals, respectively [58]

The organometallic thiocyanate crystals are optically transparent in the entire visible region making them a promising candidate for optical applications. The SHG efficiency of various organometallic thiocyanate crystals was discussed in this section to give a complete insight into it.

3.7. Dielectric studies

Dielectric measurement is one of the useful characterizations for studying the electrical response of materials, which provide information about the electric field distribution within materials. By studying the variation of the dielectric constant as a function of frequency and temperature, one can understand the different polarization mechanisms in solid such as atomic polarization of lattice, orientation polarization of dipoles, space charge polarization, electric and ionic polarizations [72].

Dielectric studies of different organometallic thiocyanate crystals were carried out using a dielectric constant measurement instrument. The experimental setup basically consists of two parallel plate capacitors and the polished graphite/silver coated sample will be placed between two electrodes. Usually, the capacitance of the sample can be measured by varying the frequency from few Hertz to few Megahertz say for example from 100 Hz to 5 MHz. The graph plotted for dielectric constant (ε') versus applied frequency yield information about dielectric properties of the materials. It is noteworthy that the dielectric constant of all the organometallic thiocyanate crystals shows higher value in the lower frequency region and decreases with the increase in applied frequency. The phenomenon of decreasing the dielectric constant with the increase in frequency is known as anomalous dielectric dispersion.

According to the Miller rule, the optimization of the SHG coefficient can be achieved by the lower value of dielectric constant [23]. Temperature plays a role in determining the values of the dielectric constant. At higher temperatures, the dielectric constant is large and is attributed to the blocking of charge carriers at the electrodes [73]. This impedance to the motion of charge carriers at the electrode leads to space charge and microscopic distribution which causes the large value of dielectric constant at lower frequencies.

Since the materials having low dielectric constant contains less number of dipoles per unit volume, these materials possess less dielectric loss compared to the material exhibiting higher dielectric constant. In general, the crystals with fewer defects will possess very low dielectric loss at low frequencies and such kind of crystals is very good for the applications like high-speed electro-optic modulators (broadly for NLO applications) [73].

The dielectric constant (ε') and dielectric loss (ε'') were calculated from the following equations;

$$\varepsilon' = \frac{Ct}{\varepsilon_{\circ} A} \tag{31}$$

$$\varepsilon'' = \varepsilon' D \tag{32}$$

where ε_0 is the permittivity of free space, t is the thickness of the sample, D is the dissipation factor and A is the area of the cross-section of the sample [72].

As an example, variation in the dielectric constant and dielectric loss as a function of temperature and frequency for MMTC crystal are shown in Fig. 7 [19]. There exists a close relationship on the behavior of the crystal under both the electric field and the laser light irradiation. This allows studying the power dissipation factor from dielectric studies. A crystal having high dielectric constant values lead to power dissipation [74]. The dielectric constant of the material is due to the contribution of frequency dependent electric, ionic, orientation and space charge polarization. The low dielectric loss at higher frequencies is attributed to the inequality in electric wave frequency and natural frequency of the bounded charges, leading to very weak radiation.

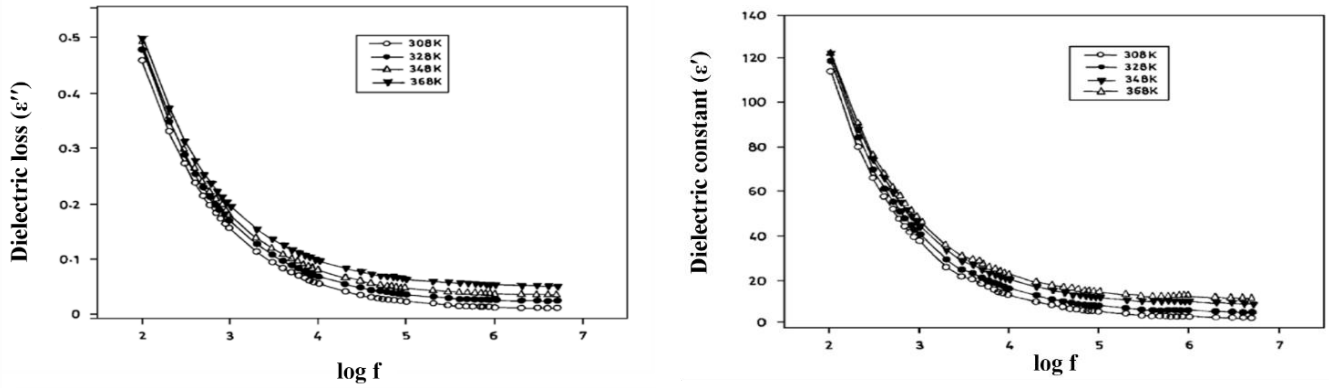

(a) Dielectric loss (b) Dielectric constant

Fig. 7 Variation with respect to the applied frequencies [19]

3.8. Surface laser damage threshold measurement

Laser Damage Threshold (LDT) is an important aspect for the non-linear optical crystals. It is meant to determine the laser damage threshold of pulse fluency or laser intensity below which no damage is likely to occur. Absorption driven and dielectric break-down damage are the two broadly classified laser damages. Depending on the material properties like absorption coefficient, specific heat, melting temperature, as well as defects that cause scattering and concentrated electric field effects, geometrical properties of a sample like thickness, homogeneity, surface morphology etc., and indeed the properties of the laser beam itself can conclude which type is dominant.

The condition under which the laser damage is expected to occur by long-pulse laser and quasi-CW laser is

$$\frac{P_{avg}}{R(\pi)(diameter^2)} > \frac{\lambda}{\lambda_{spce}}\left[\sqrt{\frac{\tau}{\tau_{spce}}(LDT_{LP})}\right] \tag{33}$$

and

$$\frac{P_{avg}}{\pi/4(diameter^2)} > 10000\left(\frac{W}{J}\right)\left(\frac{\lambda}{\lambda_{spce}}\right)LDT_{LP} \tag{34}$$

respectively (The CW and quasi-CW laser, cases are rough estimations, and should not be taken as guaranteed specifications). In case of CW type laser, the LDP may occur when

$$\frac{P_{avg}}{\pi/4(diameter^2)} > 10000\left(\frac{W}{J}\right)\left(\frac{\lambda}{\lambda_{spce}}\right)LDT_{LP} \tag{35}$$

The pulse duration (τ) is in a nano second to microsecond for large pulse laser and is in femtosecond to picosecond in case of a quasi-CW laser, whereas the repetition rate (R) is almost same for both the lasers and it varies from 1 to 100Hz.

Explicitly the laser damage threshold for the desired material can be calculated by the equation [56].

$$I = \frac{P}{S} = \frac{E}{tS} = \frac{E}{t\frac{\pi d^2}{4}} = \frac{4E}{t\pi d^2} \tag{36}$$

where I and P are the power density and power of incident light, respectively, E is single pulse energy, t is pulse width, S and d are area and diameter of the spot respectively.

The selected surface of single crystals is normally polished with a fine polishing sheet in order to form the uniform surface quality. The single-shot surface laser damage threshold was estimated using a Q-switched Nd-YAG laser of wavelength 1064 nm with a pulse width of 10 to 20 ns and 10Hz repetition rate. Few of the organometallic thiocyanate crystals were also subjected to the laser damage threshold studies and the reported results were tabulated in Table 6.

Table 6 Laser damage threshold of few well known organometallic thiocyanate crystals with KDP and Urea as reference

Crystal	Laser damage threshold (GW/cm2)	Ref.
MMTC	15.9 (1064 nm, 10 ns)	[75]
CMTC	4.59 (1064 nm, 10 ns)	[42]
ZCTC	6.24 (1064 nm, 10 ns)	[30]
MMTN	225.7 (1064nm, 10ns)	[56]
KDP	14.4 (1064 nm, 12 ns, 30_m)	[56]
Urea	5 (1064 nm, 10 ns)	[56]

3.9. Third-ordernonlinear optical properties

The quantitative information about the nonlinear optical properties of crystals is necessary for its efficient usage as NLO devices. The development of high power laser sources led to the possibility of measuring these properties [5, 9-11, 17, 20, 75]. The Z-scan technique developed by Sheik-Bahae et al. can be used to characterize the third-order nonlinear optical property of the material which readily provides the magnitude and sign of the nonlinearity. Though the third order NLO property was not extensively studied, it is worth discussing here for at least the reported organometallic thiocyanate crystal.

The Z-scan technique works on the principle of spatial beam distortion and the technique is outstanding in terms of simplicity as well as very high sensitivity for distinguishing the contribution of real and imaginary part (nonlinear refraction and absorption respectively) of third-order nonlinear susceptibility χ^3.

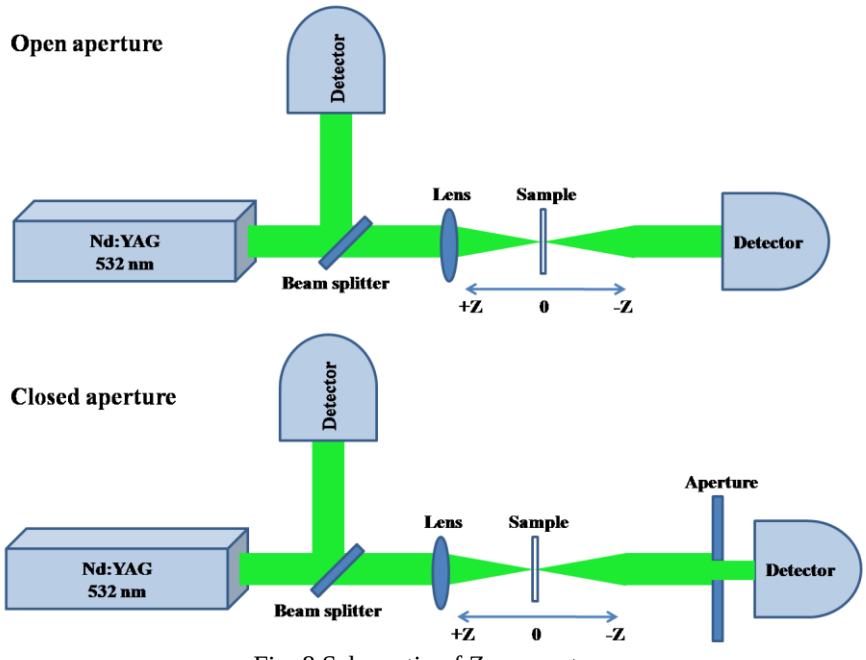

Fig. 8 Schematic of Z-scan setup

For measuring the refractive nonlinear property and non-linear absorption, a combination of an aperture and a beam splitter setup is employed in front of two detectors, which were mounted perpendicular to each other. The schematic is shown in Fig. 8. The transmittance of the laser beam through the sample is recorded as a function of sample position on Z-axis from both the detectors (one as closed aperture and one as open aperture Z-scan). The sample is fixed across the focal regime along the axial direction of the propagation of the laser beam. The transmitted beam can be measured using photodetector and digital power meter. Depending on whether nonlinear refraction is positive or negative, the sample causes focusing or defocusing within the material.

By fitting the experimental open and closed aperture Z-scan data, the non-linear absorption coefficient and the non-linear refractive index of the sample can be determined. The ratio of the measured signals of closed to open aperture is used to determine the nonlinear refraction of the sample. The different nonlinear parameters of reported MMTC single crystal are tabulated in Table 7.

Table 7 Optical third order nonlinearity data of MMTC single crystal [75]

S. No.	Parameters	MMTC
1	$\Delta\phi$	0.11
2	$n_2(cm^2/W)$	-63.3
3	$\beta(cm/W)$	2.71×10^{-6}
4	$\mathrm{Im}\,\chi^{(3)}(esu)$	2.77×10^{-8}
5	$\mathrm{Re}\,\chi^{(3)}(esu)$	0.823×10^{-9}
6	$\chi^{(3)}(esu)$	3.13×10^{-8}

The insight analytical steps for determining the third-order nonlinear optical parameters are discussed in the following steps. The spatial distribution of the temperature in the crystal surface is produced when the crystalline sample is exposed to the laser beam. This is because the localized absorption of a tightly focused beam starts propagating through the absorbing sample. Hence, a spatial variation of the refractive index is produced which acts as a thermal lens resulting in the face distortion of the propagating beam [6-17].

The peak and valley transmission difference (ΔT_{p-v}) is given in terms of an axis phase shift at the focus as

$$\Delta T_{p-v} = 0.406(1-S)^{0.25|\Delta\phi|} \tag{37}$$

where S is linear transmittance of aperture and that can be calculated from the relation

$$S = 1 - Exp\left(-2r_a^2 \Big/ \omega_a^2\right) \tag{38}$$

where ra is aperture radius and ωa beam radius at the aperture.

The nonlinear refractive index n_2 can be calculated by the formula

$$n_2 = \frac{\Delta\phi}{KI_\circ L_{eff}} \tag{39}$$

where $K = 2\pi/\lambda$ (λ is the wavelength of the laser), I_0 is the intensity of the laser beam at the focus (z=0), $L_{eff} = [1 - Exp(-\alpha L)/\alpha]$ is the effective thickness of the sample, α is the linear absorption, Δϕ is the on-axis phase shift and L is the thickness of the sample.

From the open aperture Z-scan data, the nonlinear absorption coefficient (β) is estimated by the following equation

$$\beta = \frac{2\sqrt{2\Delta T}}{I_\circ L_{eff}} \tag{40}$$

where ΔT is the one valley value at the open aperture Z-scan curve. For saturable absorption, the value of β is negative whereas for two-photon absorption it will be positive.

The real and imaginary part of the third order nonlinear optical susceptibility is defined by the following equations

$$\begin{aligned} \mathrm{Re}\,\chi^3(esu) &= \frac{10^{-4}(e_\circ C^2 n^2 n_2)}{\pi}(cm^2/W) \\ \mathrm{Im}\,\chi^3(esu) &= \frac{10^{-2}(e_\circ C^2 n^2 \lambda\beta)}{4\pi^2}(cm/W) \\ \left|\chi^{(3)}\right| &= \sqrt{(\mathrm{Re}\,\chi^3)^2 + (\mathrm{Im}\,\chi^3)^2} \end{aligned} \tag{41}$$

where $\varepsilon_\circ$ is vacuum permittivity, $n_\circ$ is the linear refractive index of the sample and C is the velocity of light in vacuum. It is worth mentioning here that the nonlinear index of refraction is proportional to the Re(χ^3) and the nonlinear absorption coefficient is proportional to the imaginary part of the third order susceptibility $\mathrm{Im}(\chi^3)$.

Comparative study of reported third-order nonlinear susceptibility data of organic as well as organometallic crystals, for example, KDP (1.7×10-14 esu), BBO (5.7×10-14 esu) and MMTC (6.58×10-9 eus) reveal the fact that the organometallic crystal has a much higher value of χ^3. In fact, it is quite natural that the presence of an organic ligand (SCN-) with its small π-electron systems encourages more dominant NLO effect. π-electron delocalization has been assumed to be the source of large χ^3 in conjugated molecules. It is also reported that the value of χ^3 for these crystals is larger than some of the polymers which are well studied for their NLO properties. In contrast, the influence of the organic ligand in modifying the second and third order NLO properties of organometallic was confirmed by the review on the third order nonlinear optical susceptibility [75-76].

3.10. Optical limiting

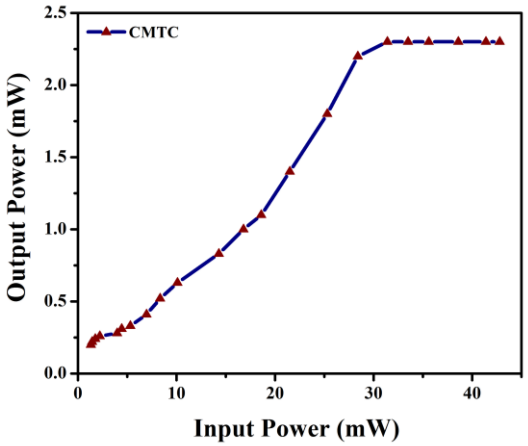

Fig. 9 Optical limiting behavior of CMTC crystal [70]

Optical limiting behavior can be observed in the materials that exhibit at least one among the nonlinear absorption, induced scattering, nonlinear refraction,and even phase transitions. Such materials can be used to protect the sensors and human eye from the high power lasers. Limiting threshold is a quantity defined as the input energy at which the transmittance is 50% of the linear transmittance which decides the goodness of material to use it in an optical limiting devices. Lower the optical limiting threshold, better the optical limiting material. Use of a polarized-analyzer combination to vary the input power in a Z-scan instrument can be an experimental setup to characterize the optical limiting behavior of a material. By varying the input power, the corresponding output power was recorded. The optical liming threshold of the CMTC single crystal is 31.2 mW. As an example, the optical limiting behavior of the CMTC crystal is shown in Fig. 9 [70].

Presence of transition metal atoms in organometallic thiocyanate compounds increases the optical transition in the system due to d-d electron transition. Generally, metal-ligand and intra-ligand transitions could be possible. These transitions lead to a separation of charge and, hence, coupled significantly to an applied optical electric field. This kind of coupling yields a very high extinction coefficient which is one of the fundamental requirements for optical limiting. Therefore, organometallic thiocyanate crystals can be a promising candidate for optical limiting devises.

4. Conclusions

The basic need of bimetallic thiocyanate crystal is to achieve good optoelectronic properties as exhibited by organic materials and to achieve good mechanical properties like inorganic materials. In that vision, numerous families of crystals were grown and analyzed among which thiocyanate crystal family is remarkable. The Zinc Cadmium Thiocyanate (ZCTC) single crystals and the crystals from its Lewis based addicts were extensively studied crystal material in the family of bimetallic thiocyanate single crystals. The synthesis and growth of the majority of the compounds belonging to the thiocyanate family have been discussed in detail. Among them, materials like MMTC, ZMTC, ZCTC, CMTC, etc., were studied extensively in the last few years and many are yet to study. Various characterization techniques were used to understand these materials in detail. We made an effort to bring a collective, quantitative and qualitative data available in the literature regarding organometallic thiocyanate crystals.

Conflicts of Interest

The authors declare no conflict of interest.

Acknowledgment

Authors acknowledge support from DAE-BRNS, Government of India, though the Project Ref. No.-34/14/55/2014-BRNS/2014 during the course of this work.

References

[1] X. Q. Wang et al., “Growth and characterization of a novel UV nonlinear optical crystal: [MnHg $(SCN)_4(H_2O)_2]\cdot 2C_4H_9NO$,” Journal of crystal growth, vol. 234, pp. 469-479, 2002.

[2] X. Q. Wang, D. Xu, M. K. Lu, D. R. Yuan, and S. X. Xu, “Crystal growth and characterization of the organometallic nonlinear optical crystal: manganese mercury thiocyanate (MMTC),” Materials research bulletin, vol. 36, pp. 879-887, 2001.

[3] X. Q. Wanget al., “Crystal growth and characterization of a novel organometallic nonlinear-optical crystal: MnHg(SCN)4(C2H6OS)2,” Journal of crystal growth, vol. 224, pp. 284-293, 2001.

[4] X. Q. Wanget al., and M. H. Jiang, “Synthesis, structure and properties of a new nonlinear optical material: zinc cadmium tetrathiocyanate,” Materials Research Bulletin, vol. 34, pp. 2003-2011, 1999.

[5] P. V. Dhanaraj, N. P. Rajesh, J. K. Sundar, S. Natarajan, and G. Vinitha, “Studies on growth, crystal structure and characterization of novel organic nicotinium trifluoroacetate single crystals,” Materials Chemistry and Physics, vol. 129, pp. 457-463, 2011.

[6] P. V. Dhanaraj, N. P. Rajesh, G. Vinitha, and G. Bhagavannarayana, “Crystal structure and characterization of a novel organic optical crystal: 2-Aminopyridinium trichloroacetate,” Materials Research Bulletin, vol. 46, pp. 726-731, 2011.

[7] S. Dhanuskodi, T. C. S. Girisun, and S. Vinitha, “Optical limiting behavior of certain thiourea metal complexes under CW laser excitation,” Current Applied Physics, vol. 11, pp. 860-864, 2011.

[8] T. C. S. Girisun, S. Dhanuskodi, and G. Vinitha, “$\chi(3)$ measurement and optical limiting properties of metal complexes of thiourea using Z-scan,” Materials Chemistry and Physics, vol. 129, pp. 9-14, 2011.

[9] R. M. Jauhar, V. Viswanathan, P. Vivek, G. Vinitha, D. Velmurugan, and P. Murugakoothan, “A new organic NLO material isonicotinamidium picrate (ISPA): crystal structure, structural modeling and its physico-chemical properties,” RSC Advances, vol. 6, pp. 57977-57985, 2016.

[10] R. P. Jebin, T. Suthan, N. P. Rajesh, G. Vinitha, and S. A. B. Dhas, "Studies on crystal growth and physical properties of 4-(dimethylamino) benzaldehyde-2, 4-dinitroaniline single crystal," Optical Materials, vol. 57, pp. 163-168, 2016. (https://www.sciencedirect.com/science/article/pii/S0925346716302117)

[11] R. P. Jebin, T. Suthan, N. P. Rajesh, G. Vinitha, and U. Madhusoodhanan, "Growth and characterization of organic material 4-dimethylaminobenzaldehyde single crystal," Spectrochimica Acta Part A: Molecular and Biomolecular Spectroscopy, vol. 135, pp. 959-964, 2015.

[12] D. Mahendiran, G. Vinitha, S. Shobana, V. Viswanathan, D. Velmurugan, and A. K. Rahiman, "Theoretical, photophysical and biological investigations of an organic charge transfer compound2-aminobenzimidazolium-2-oxyisoindolate-1, 3-dione-2-hydroxyisoindoline-1, 3-dione," RSC Advances, vol. 6, pp. 60336-60348, 2016.

[13] T. Thilak, M. B. Ahamed, G. Marudhu, and G. Vinitha, "Effect of KDP on the growth, thermal and optical properties of L-alanine single crystals," Arabian Journal of Chemistry, vol. 9, pp. 676-680, 2016.

[14] S. Venda, G. Peramaiyan, M. NizamMohideen, G. Vinitha, and S. Srinivasan, "Synthesis, growth, structural, thermal, dielectric, linear and nonlinear optical studies of 2-amino 6-methylpyridinium salicylate single crystal," Journal of Optics, vol. 46, pp. 149-157, 2017.

[15] C. Vesta, R. Uthrakumar, G. Vinitha, A. Ramalingam, and S. J. Das, "Studies on novel single crystals of tri-nitrophenol methyl p-hydroxybenzoate," Journal of Crystal Growth, vol. 311, pp. 4016-4021, 2009.

[16] A. Vijayalakshmi, V. Balrajand, and G. Vinitha, "Structure and characterization of a new organic crystal for optical limiting applications, isonicotinamide bis-p-aminobenzoic acid," Ukr. J. Phys. Opt, vol. 17, p. 99, 2016.

[17] A. Vijayalakshmi, B. Vidyavathy, and G. Vinitha, "Crystal structure, growth and nonlinear optical studies of isonicotinamide p-nitrophenol: A new organic crystal for optical limiting applications," Journal of Crystal Growth, vol. 448, pp. 82-88, 2016.

[18] Z. Blank, "The growth of cadmium mercury thiocyanate and zinc mercury thiocyanate crystals in gels," Journal of Crystal Growth, vol. 18, pp. 281-288, 1973.

[19] G. P. Josephet al., "Growth and characterization of an organometallic nonlinear optical crystal of manganese mercury thiocyanate (MMTC)," Journal of crystal growth, vol. 296, pp. 51-57, 2006.

[20] M. Mahadevan, P. K. Sankar, G. Vinitha, M. Arivanandhan, K. Ramachandran, and P. Anandan, "Non linear optical studies on semiorganic single crystal: L-arginine 4-nitrophenalate 4-nitrophenol dihydrate (LAPP)," Optics & Laser Technology, vol. 92, pp. 168-172, 2017.

[21] D. R. Yuanet al., "Growth of cadmium mercury thiocyanate single crystal for laser diode frequency doubling," Journal of crystal growth, vol. 186, pp. 240-244, 1998.

[22] I. V. Potheher, J. Madhavan, K. Rajarajan, K. Nagaraja, and P. Sagayaraj, "Growth and characterization of diaquatetrakis (thiocyanato) cobalt (II) mercury (II) N-methyl-2-pyrolidone (CMTWMP) single crystals," Journal of Crystal Growth, vol. 310, pp. 124-130, 2008.

[23] C. Raghavan, R. Sankar, R. Mohankumar, and R. Jayavel, "Synthesis, growth and characterization of nonlinear optical diaqua (thiocyanato) manganese mercury-N, N-dimethylacetamide single crystals," Journal of Crystal Growth, vol. 311, pp. 1346-1351, 2009.

[24] X. Q. Wanget al., "Growth morphology and properties of the organometallic nonlinear optical crystal [MnHg(SCN)4(H2O)2]·2C4H9NO," physica status solidi (a), vol. 198, pp. 43-48, 2003.

[25] X. Q. Wanget al., "Polymeric diaquatetra-μ-thiocyanato-manganese (II) mercury (II) bis (N, N-dimethylacetamide) solvate," Acta Crystallographica Section C: Crystal Structure Communications, vol. 56, pp. 1305-1307, 2000.

[26] S. Chandralingam, A. K. Augustine, G. Sreekanth, and G. P. Joseph, "Synthesis, optical and dielectric properties of highly efficient organobimetallic thiocyanate complex crystals," in IOP Conference Series: Materials Science and Engineering, p. 012003, 2013.

[27] X. Q. Wanget al., "A systematic spectroscopic study of four bimetallic thiocyanates of chemical formula AB(SCN)4: ZnCd(SCN)4 and AHg (SCN)4 (A= Zn, Cd, Mn) as UV nonlinear optical crystal materials," Optical Materials, vol. 23, pp. 335-341, 2003.

[28] X. Q. Wang,et al., "Investigation of bimetallic thiocyanates belonging to ABTC structure type: ZnCd(SCN)4 and AHg(SCN)4 (A= Zn, Cd, Mn) as nonlinear optical crystal materials," Crystal Research and Technology: Journal of Experimental and Industrial Crystallography, vol. 36, pp. 73-84, 2001.

[29] X. Q. Wanget al., "Crystal growth and characterization of a new organometallic nonlinear optical crystal material: MnHg(SCN)4(C3H8O2)," physica status solidi (a), vol. 191, pp. 106-116, 2002.

[30] X. Q. Wanget al., "Investigation on growth and macro-defects of a UV nonlinear optical crystal: ZnCd(SCN)4," Journal of crystal growth, vol. 235, pp. 340-346, 2002.

[31] P. M. Ushasree, R. Jayavel, C. Subramanian, and P. Ramasamy, "Growth of zinc thiourea sulfate (ZTS) single crystals:: a potential semiorganic NLO material," Journal of crystal growth, vol. 197, pp. 216-220, 1999.

[32] P. V. Dhanaraj, G. Bhagavannarayana, and N. P. Rajesh, "Effect of amino acid additives on crystal growth parameters and properties of ammonium dihydrogen orthophosphate crystals," Materials Chemistry and Physics, vol. 112, pp. 490-495, 2008.
[33] K. Sangwal, "On the estimation of surface entropy factor, interfacial tension, dissolution enthalpy and metastable zone-width for substances crystallizing from solution," Journal of crystal growth, vol. 97, pp. 393-405, 1989.
[34] N. P. Zaitseva, L. N. Rashkovich, and S. V. Bogatyreva, "Stability of KH2PO4 and K(H,D)2PO4 solutions at fast crystal growth rates," Journal of Crystal Growth, vol. 148, pp. 276-282, 1995.
[35] G. Arunmozhi, R. M. Kumar, R. Jayavel, and C. Subramanian, "Growth and surface studies on triglycine sulpho-phosphate (TGSP) single crystals," Materials Science and Engineering: B, vol. 49, pp. 216-220, 1997.
[36] P. M. Ushasree, R. Muralidharan, R. Jayavel, and P. Ramasamy, "Growth of bis (thiourea) cadmium chloride single crystals-a potential NLO material of organometallic complex," Journal of crystal growth, vol. 218, pp. 365-371, 2000.
[37] N. Kubota, J. Fukazawa, H. Yashiro, and J. W. Mullin, "Impurity effect of chromium (III) on the growth and dissolution rates of potassium sulfate cyrstals," Journal of crystal growth, vol. 149, pp. 113-119, 1995.
[38] R. J. Usha, J. A. M. Mani, and V. Joseph, "Impedance analysis of bimetallic thiocyanate ligand based single crystals of MnHg(SCN)4 and CdHg(SCN)4," Archives of Appl. Sci. Res, vol. 4, pp. 638-644, 2012.
[39] L. B. Kumar, K. K. Murthy, Y. N. Rajeev, J. Madhavan, P. Sagayaraj, and S. Cole, "Influence of rare earth doping on the spectral, thermal, morphological, and optical properties of nonlinear optical single crystals of manganese mercury thiocyanate, MnHg(SCN)4," Optik-International Journal for Light and Electron Optics, vol. 126, pp. 4899-4904, 2015.
[40] P. Jagdish and N. P. Rajesh, "Effect of copper on the growth morphology and characterization of zinc mercury thiocyanate crystals," Journal of Industrial and Engineering Chemistry, vol. 18, pp. 2157-2161, 2012.
[41] P. N. S. Kumari, S. Kalainathan, and N. A. N. Raj, "Study of optimum growth condition and characterization of zinc mercury thiocyanate (ZMTC) single crystals in silica gel," Materials Research Bulletin, vol. 42, pp. 2099-2106, 2007.
[42] C. Raghavan, R. Pradeepkumar, G. Bhagavannarayan, and R. Jayavel, "Growth of cadmium mercury thiocyanate single crystals using acetone-water mixed solvent and their characterization studies," Journal of Crystal Growth, vol. 311, pp. 3174-3178, 2009.
[43] X. Q. Wang, D. Xu, M. K. Lu, D. R. Yuan, J. Huang, S. G. Li, G. W. Lu, H. Q. Sun, S. Y. Guo, G. H. Zhang, X. L. Duan, H. Y. Liu, and W. L. Liu, "Physicochemical behavior of nonlinear optical crystal CdHg(SCN)4," Journal of crystal growth, vol. 247, pp. 432-437, 2003.
[44] B. K. Lanka, N. R. Yerramalla, and S. Cole, "Growth and characterization of pure and rare earth doped organometallic nonlinear optical single crystals of manganese mercury thiocyanate (MMTC)," International Journal of ChemTech Research, vol. 6, pp. 1789-1791, 2014.
[45] B. K. Lanka, M. T. Madanu, N. R. Yerramalla, and S. Cole, "Spectral and optical properties of pure and rare earth doped nonlinear optical (NLO) active single crystals of manganese mercury thicocyanate bis-dimethyl sulfoxide," International journal of Engineering Research, vol. 3, pp. 15-17, 2015. (http://www.ijoer.in/Special%20Issue.html)
[46] G. P. Joseph, N. Melikechi, J. Philip, J. Madhavan, and P. Sagayaraj, "Studies on the electrical, linear and nonlinear optical properties of Manganese mercury thiocyanate bis-dimethyl sulfoxide, an efficient NLO crystal," Physica B: Condensed Matter, vol. 404, pp. 295-299, 2009.
[47] X. Q. Wanget al., "Manganese mercury thiocyanate (MMTC) glycol monomethyl ether," Acta Crystallographica Section C: Crystal Structure Communications, vol. 56, pp. 647-648, 2000.
[48] P. Paramasivam, M. Arivazhagan, and C. R. Raja, "Synthesis, growth and characterization of zinc manganese thiocyanate crystal," Indian Journal of Pure and Applied Physics, vol. 49, pp. 394-397, 2011.
[49] X. N. Jianget al., "Growth of zinc cadmium thiocyanate single crystal for laser diode frequency-doubling," Journal of crystal growth, vol. 222, pp. 755-759, 2001.
[50] K. Rajarajan et al., "Growth and optical studies of a novel organometallic complex NLO crystal: Tetrathiourea cadmium (II) tetrathiocyanato zinc (II)," Materials and manufacturing processes, vol. 22, pp. 370-374, 2007.
[51] R. Manimekalai, A. P. Raj, and C. R. Raja, "Growth and characterization of ethylene diamine tetra acetate (EDTA) doped lithium sulphate monohydrate crystals," Optics and Photonics Journal, vol. 2, p. 216, 2012.
[52] G. Pabitha and R. Dhanasekaran, "Investigation on the crystal growth and characterisation of an organometallic non linear optical crystal-Tetrathiourea mercury tetrathiocyanato manganate," Materials Science and Engineering: B, vol. 177, pp. 1149-1155, 2012.
[53] K. Rajarajan et al., "Growth, optical, dielectric and ESR studies on tetrathiourea mercury (II) tetrathiocyanato manganate (II): an organometallic complex NLO crystal," Journal of Physics and Chemistry of Solids, vol. 68, pp. 2370-2375, 2007.
[54] K. Rajarajanet al., "Growth and characterization of organometallic nonlinear optical TMTM single crystals," Journal of crystal growth, vol. 304, pp. 435-440, 2007.

[55] H. Le Bozec and T. Renouard, "Dipolar and non-dipolar pyridine and bipyridine metal complexes for nonlinear optics," European Journal of Inorganic Chemistry, vol. 2000, pp. 229-239, 2000.
[56] X. Q. Wanget al., "Single crystal growth, structural characterization, thermal and optical properties of a novel organometallic nonlinear optical crystal: MnHg(SCN)4(C2H5NO)2," Physica B: Condensed Matter, vol. 405, pp. 1071-1080, 2010.
[57] S. Guo, D. R. Yuanet al., "Growth of cadmium mercury thiocyanate dimethylsulphoxide single crystal for laser frequency doubling," Progress in crystal growth and characterization of materials, vol. 40, pp. 75-79, 2000.
[58] C. M. Raghavan, R. Sankar, R. M. Kumar, and R. Jayavel, "Growth and characterization of nonlinear optical bis-(dimethylsulfoxide) cadmium mercury thiocyanate single crystal," Journal of Crystal Growth, vol. 310, pp. 4570-4575, 2008.
[59] . S. M. R. Kumar, S. Selvakumar, and P. Sagayaraj, "Synthesis, growth and physicochemical properties of an organometallic nonlinear optical crystal: mercury cadmium chloride thiocyanate," Optik-International Journal for Light and Electron Optics, vol. 125, pp. 1071-1074, 2014.
[60] S. M. R. Kumar, N. Melikechi, S. Selvakumar, and P. Sagayaraj, "Growth and characterization of nonlinear optical bimetallic thiocyanate complex of MCCTC crystal," Journal of Crystal Growth, vol. 311, pp. 2454-2458, 2009.
[61] C. M. Raghavan, A. Bhaskaran, R. Sankar, and R. Jayavel, "Studies on the growth, structural, optical, thermal and electrical properties of nonlinear optical cadmium mercury thiocyanate glycol monomethyl ether single crystal," Current Applied Physics, vol. 10, pp. 479-483, 2010.
[62] M. Zhou, Y. F. Luo, D. Xu, S. Guo, M. K. Lu, and D. R. Yuan, "Crystal structure of cadmium mercury tetrathiocyanate (glycol monomethyl ether), C7H8CdHgN4O2S4," Zeitschrift für Kristallographie-New Crystal Structures, vol. 215, pp. 425-426, 2000.
[63] X. Q. Wanget al., "Growth, spectroscopic and thermal behavior of Cd(SCN)2(DMSO)2," Journal of crystal growth, vol. 246, pp. 155-160, 2002.
[64] B. Vijayabhaskarana, M. Arivazhagan, and C. R. Raja, "Synthesis, growth and characterization of copper mercury thiocyanate crystal," Indian Journal of Pure and Applied Physics, vol. 49, pp. 340-343, 2011.
[65] X. Q. Wanget al., "Growth and properties of UV nonlinear optical crystal ZnCd(SCN)4," Materials research bulletin, vol. 36, pp. 1287-1299, 2001.
[66] V. Ramesh, A. S. Syed, K. Jagannathan, and K. Rajarajan, "Growth, spectroscopic and physicochemical properties of bis mercury ferric chloride tetra thiocyanate: A nonlinear optical crystal," Spectrochimica Acta Part A: Molecular and Biomolecular Spectroscopy, vol. 108, pp. 236-243, 2013.
[67] G. W. Lu, H. R. Xia, X. Q. Wang, D. Xu, Y. Chen, and Y. Q. Zhou, "Raman scattering investigation of the zinc cadmium tetrathiocyanate single crystals," Materials Science and Engineering: B, vol. 87, pp. 117-121, 2001.
[68] X. Q. Wanget al., "Effects of pH and hydrogen-bonding on the growth and characterization of ZnCd(SCN)4," Journal of crystal growth, vol. 267, pp. 263-269, 2004.
[69] R. L. Smith and G. Sandly, "An accurate method of determining the hardness of metals, with particular reference to those of a high degree of hardness," Proceedings of the Institution of Mechanical Engineers, vol. 102, pp. 623-641, 1922.
[70] T. A. Hegde, A. Dutta, and G. Vinitha, "$\chi(3)$ measurement and optical limiting behaviour of novel semi-organic cadmium mercury thiocyanate crystal by Z-scan technique," Applied Physics A, vol. 124, pp. 808 (1-10), 2018.
[71] R. M. Kumar, D. R. Babu, D. Jayaraman, R. Jayavel, and K. Kitamura, "Studies on the growth aspects of semi-organic L-alanine acetate: a promising NLO crystal," Journal of Crystal Growth, vol. 275, pp. e1935-e1939, 2005.
[72] R. J. Usha, P. Sagayaraj, and V. Joseph, "Linear and nonlinear optical, mechanical, electrical and surface studies of a novel nonlinear optical crystal-Manganese mercury thiocyanate (MMTC)," Spectrochimica Acta Part A: Molecular and Biomolecular Spectroscopy, vol. 133, pp. 241-249, 2014.
[73] S. K. Arora, V. Patel, B. Amin, and A. Kothari, "Dielectric behaviour of strontium tartrate single crystals," Bulletin of Materials Science, vol. 27, pp. 141-147, 2004.
[74] L. R. Dalton, "Rational design of organic electro-optic materials," Journal of Physics: Condensed Matter, vol. 15, pp. R934, 2003.
[75] T. R. Kumar, R. J. Vijay, R. Jeyasekaran, S. Selvakumar, M. A. Arockiaraj, and P. Sagayaraj, "Growth, linear and nonlinear optical and, laser damage threshold studies of organometallic crystal of MnHg(SCN)4," Optical Materials, vol. 33, pp. 1654-1660, 2011.
[76] H. S. Nalwa, "Organometallic materials for nonlinear optics," Applied organometallic chemistry, vol. 5, pp. 349-377, 1991.